

Energy spectra of fractional quantum Hall systems in the presence of a valence hole

Arkadiusz Wójs

*Department of Physics, University of Tennessee, Knoxville, Tennessee 37996
Institute of Physics, Wrocław University of Technology, Wrocław 50-370, Poland*

John J. Quinn

Department of Physics, University of Tennessee, Knoxville, Tennessee 37996

The energy spectrum of a two-dimensional electron gas (2DEG) in the fractional quantum Hall regime interacting with an optically injected valence band hole is studied as a function of the filling factor ν and the separation d between the electron and hole layers. The response of the 2DEG to the hole changes abruptly at d of the order of the magnetic length λ . At $d < \lambda$, the hole binds electrons to form neutral (X) or charged (X^-) excitons, and the photoluminescence (PL) spectrum probes the lifetimes and binding energies of these states rather than the original correlations of the 2DEG. The “dressed exciton” picture (in which the interaction between an exciton and the 2DEG was proposed to merely enhance the exciton mass) is questioned. Instead, the low energy states are explained in terms of Laughlin correlations between the constituent fermions (electrons and X^- 's) and the formation of two-component incompressible fluid states in the electron-hole plasma. At $d > 2\lambda$, the hole binds up to two Laughlin quasielectrons (QE) of the 2DEG to form fractionally charged excitons hQE_n . The previously found “anyon exciton” hQE_3 is shown to be unstable at any value of d . The critical dependence of the stability of different hQE_n complexes on the presence of QE's in the 2DEG leads to the observed discontinuity of the PL spectrum at $\nu = \frac{1}{3}$ or $\frac{2}{3}$.

71.35.Ji, 71.35.Ee, 73.20.Dx

I. INTRODUCTION

A number of experimental^{1–20} and theoretical^{21–37} studies of the optical properties of quasi-two-dimensional (2D) electron systems in high magnetic fields have been carried out in the recent years. In structures where both conduction electrons and valence holes are confined in the same 2D layer, such as symmetrically doped quantum wells (QW's), the photoluminescence (PL) spectrum of an electron gas (2DEG) involves neutral and charged exciton complexes (bound states of one or two electrons and a hole, $X = e-h$ and $X^- = 2e-h$).^{10–20,29–35} The X^- can exist in the form of a number of different bound states. In zero or low magnetic field ($B \leq 2$ T in GaAs), only the optically active spin-singlet X_s^- occurs.^{29,34,35} Although it is predicted to unbind in the $B \rightarrow \infty$ limit as a consequence of the “hidden symmetry” of an $e-h$ system in the lowest LL,^{21–23} the X_s^- is observed in the PL spectra even in the highest fields available experimentally (~ 50 T in GaAs).¹⁴ A different X^- bound state is formed in a finite magnetic field: a non-radiative (“dark”) spin-triplet X_{td}^- .^{12,13} In contrast with an earlier prediction,²³ the X_{td}^- remains bound in the $B \rightarrow \infty$ limit,^{30,31} and the transition from the X_s^- to the X_{td}^- ground state is expected at $B \approx 30$ T (in GaAs).^{34,35} At even higher fields, Laughlin incompressible fluid states of strongly bound and long-lived X_{td}^- fermionic quasiparticles were predicted.^{32,33} Very recently, yet another bound X^- state has been discovered³⁴ in a strong (but finite) magnetic field: a radiative (“bright”) excited spin-triplet X_{tb}^- . The X_{tb}^- has the smallest binding energy but the largest oscillator strength of all X^- states, and domi-

nates the PL spectrum at very high magnetic fields.¹⁴

The PL spectra of symmetric QW's are not very useful for studying the $e-e$ correlations in the 2DEG. In such systems, the 2DEG responds so strongly to the perturbation created by an optically injected hole that the original correlations are locally (in the vicinity of the hole) completely replaced by the $e-h$ correlations describing an X or X^- bound state. The PL spectra containing more information about the properties of the 2DEG itself are obtained in bi-layer systems, where the spatial separation of electrons and holes reduces the effects of $e-h$ correlations.²⁴ The bi-layer systems are realized experimentally in heterojunctions and asymmetrically doped wide QW's, in which a perpendicular electric field causes separation of electron and hole 2D layers by a finite distance d . Unless d is smaller than the magnetic length λ , the PL spectra of bi-layer systems show no recombination from X^- states. Instead, they show anomalies^{1–7} at the filling factors $\nu = \frac{1}{3}$ and $\frac{2}{3}$, at which Laughlin incompressible fluid states³⁸ are formed in the 2DEG, and the fractional quantum Hall (FQH) effect³⁹ is observed in transport experiments.

The bi-layer $e-h$ system can be viewed as an example of a more general one in which the 2DEG with well defined correlations (e.g., Laughlin correlations at $\nu = \frac{1}{3}$) is perturbed by a potential V_{UD} of an additional charge (mobile, in case of a valence hole), with controlled characteristic strength (energy scale) U and range (length scale) D . Although the layer separation d is the only adjustable parameter in an $e-h$ system, larger control over both U and D is possible by replacing the hole with a sharp electrode whose potential and distance from the

2DEG can be tuned independently, as in a scanning tunneling microscope (STM).⁴⁰ In another similar system, a charged impurity can be located at a controlled distance from the 2DEG.^{18,41,42} The 2DEG has its own characteristic lengths and energies, such as the average distance ($\sim \varrho^{-1/2} = \lambda\sqrt{2\pi/\nu}$) and Coulomb energy of a pair of nearest electrons, or the energy gap $\varepsilon_{\text{QE}} + \varepsilon_{\text{QH}}$ to create Laughlin quasiparticle excitations and the average separation between them. Therefore, different types of response of the 2DEG to a perturbation V_{UD} are expected depending on the relation between U and D , and the characteristic lengths and energies of the 2DEG.

Although the properties of bi-layer e - h systems in the FQH regime have been extensively studied in the past,^{23–28} the existing theory is by no means satisfactory. For example, we argue that the suggestive concept of a “dressed exciton”^{25,26} at small d is not valid, and that the “anyon exciton”²⁷ is not the relevant quasiparticle for description of the PL spectra at large d . In the present work, the elementary (“true”) quasiparticles (TQP’s) of the e - h system are identified at an arbitrary layer separation d . A unified description of the response of the 2DEG to the perturbing potential of an optically injected hole is proposed, and a transition²⁴ from an e - h correlated (excitonic) to an e - e correlated (Laughlin) phase at $d \approx 1.5\lambda$ is confirmed. This transition has a pronounced effect on the optical spectra: at larger d , the discontinuities occur at $\nu = \frac{1}{3}$ and $\frac{2}{3}$ which allow for the optical probing of the Laughlin correlations in the 2DEG.

At small layer separations ($d < \lambda$), we show that the lowest energy band of e - h states does not describe a magnetoexciton dispersion,²³ and that the “dressed exciton” model proposed by Wang et al.²⁵ and by Apalkov and Rashba²⁶ is not valid. Instead, the formation of (two-component) incompressible fluid^{33,38,43} e - X^- states in an e - h plasma is demonstrated. The states previously misinterpreted as the dispersion of a “dressed exciton” with an enhanced mass are shown to contain an X^- interacting with a quasihole (QH) of such incompressible fluid. The list of possible bound states (TQP’s) of the system at $d < \lambda$ includes the X state, different X^- states, and the X^- -QH $_n$ states in which one or two QH’s of the e - X^- fluid are bound to an X^- . Which of the TQP’s occur at the lowest energy depends critically on d and ν .

The dependence of the excitation energy gap of the incompressible e - X^- states on d is also studied. The enhancement of the gap at small $d > 0$ is predicted for some states. Combining the present result with Ref. 34 we find that Laughlin e - X^- correlations, which isolate the X^- ’s from the surrounding 2DEG, survive (or are enhanced) at small d for all of X_s^- , X_{td}^- , and X_{tb}^- states. Hence, the understanding of the PL spectra in terms of weakly perturbed X^- states remains valid at $d < \lambda$.

At large layer separations ($d > 2\lambda$), following the work of Chen and Quinn,²⁸ we study the formation and properties of fractionally charged excitons (FCX’s), or “anyonic ions,” $h\text{QE}_n$ consisting of n Laughlin quasielectrons (QE) of the 2DEG bound to a distant hole. We

give a detailed analysis of all FCX complexes in terms of their angular momenta and binding energies. The pseudopotentials^{44,45} (pair energy as a function of pair angular momentum) describing interactions between the hole, electrons, and the Laughlin quasiparticles are calculated. Using the knowledge of the involved interactions we predict the stability of $h\text{QE}$ and $h\text{QE}_2$ complexes and explain the behavior of their binding energy on the layer separation d . Somewhat surprisingly, the $h\text{QE}_3$ complex is found unstable at any value of d .

The general analysis sketched above is illustrated with the energy spectra obtained in large-scale numerical diagonalization of finite systems on a Haldane sphere.^{49,50} Using Lanczos-based algorithms⁵¹ we were able to calculate the exact spectra of up to nine electrons and a hole at the filling factors $\nu \approx \frac{1}{3}$. Since our numerical results obtained for fairly large systems can serve as raw “experimental” input for further theories, we discuss them in some detail the last section. They agree with all our predictions made throughout the paper.

Although in the present work we study a very ideal e - h system in the lowest LL, our most important conclusions are qualitative and thus apply without change to realistic systems. To obtain a better quantitative agreement with particular experiments, the effects due to the LL mixing (less important at $d \geq 2\lambda$) and finite QW widths must be included in a standard way (see, e.g., Ref. 34 for $d = 0$). Some of our conclusions should also shed light on the physics of other related systems, such as the STM. In particular, the screening of a potential of a sharp electrode by a 2DEG is expected to involve “real” electrons when U is large and D is small, and Laughlin quasiparticles in the opposite case. An asymmetry between the response of a 2DEG to a positively and negatively charged electrode is expected in the latter case, because of very different QE–QE and QH–QH interactions at short range. Let us also add that the problem at $\nu = \frac{2}{3}$ is equivalent to that at $\nu = \frac{1}{3}$ because of the charge-conjugation symmetry in the lowest LL.

The presented identification of bound states (X , X^- , X^- -QH $_n$, and $h\text{QE}_n$) in e - h systems at an arbitrary d and the study of their mutual interactions is necessary for the correct description of the PL from the 2DEG in the FQH regime. While the complete discussion of the optical properties of all bound e - h states will be presented in a following publication,⁴⁶ let us mention that the translational invariance of a 2DEG results in strict optical selection rules for bound states (analogous to those forbidding emission from an isolated X_{td}^- ^{31–33}). As a result, h (the “uncorrelated hole” state), $h\text{QE}^*$ (an excited state of an h -QE pair), and $h\text{QE}_2$ are the only stable radiative states at large d , while the recombination of $h\text{QE}$ (the ground state of an h -QE pair) or of (unstable) $h\text{QE}_3$ is forbidden. Different optical properties of different $h\text{QE}_n$ complexes and the critical dependence of their stability on the presence of QE’s in the 2DEG explain the discontinuities observed^{1–7} in the PL at $\nu = \frac{1}{3}$ or $\frac{2}{3}$.

II. MODEL

We consider a system in which a 2DEG in a strong magnetic field B fills a fraction $\nu < 1$ of the lowest LL of a narrow QW. A dilute 2D gas of valence-band holes ($\nu_h \ll \nu$) is confined to a parallel layer, separated from the electron one by a distance d . The widths of electron and hole layers are set to zero (finite widths can be included through appropriate form-factors reducing the effective 2D interaction matrix elements³⁴), and the mixing with excited electron and hole LL's is neglected. The single-particle states $|m\rangle$ in the lowest LL are labeled by orbital angular momentum, $m = 0, -1, -2, \dots$ for the electrons and $m_h = -m = 0, 1, 2, \dots$ for the holes. Since $\nu_h \ll \nu$ and no bound complexes involving more than one hole (such as biexcitons $X_2 = 2e-2h$) occur at large B , the $h-h$ correlations can be neglected and it is enough to study the interaction of the 2DEG with only one hole. The many-electron-one-hole Hamiltonian can be written as

$$H = \sum_{ijkl} \left(c_i^\dagger c_j^\dagger c_k c_l V_{ijkl}^{ee} + c_i^\dagger h_j^\dagger h_k c_l V_{ijkl}^{eh} \right), \quad (1)$$

where c_m^\dagger (h_m^\dagger) and c_m (h_m) create and annihilate an electron (hole) in state $|m\rangle$. Because of the lowest LL degeneracy, H includes only the $e-e$ and $e-h$ interactions whose two-body matrix elements V^{ee} and V^{eh} are defined by the intra- and inter-layer Coulomb potentials, $V_{ee}(r) = e^2/r$ and $V_{eh}(r) = -e^2/\sqrt{r^2 + d^2}$. The convenient units for length and energy are the magnetic length λ and the energy e^2/λ , respectively. At $d = 0$, the $e-h$ matrix elements are equal to the $e-e$ exchange ones, $V_{ijkl}^{eh} = -V_{ikjl}^{ee}$, due to the particle-hole symmetry, and at $d > 0$ the $e-h$ attraction is weaker than the $e-e$ repulsion (at short range).

The 2D translational invariance of H results in conservation of two orbital quantum numbers: the projection of total angular momentum $\mathcal{M} = \sum_m (c_m^\dagger c_m - h_m^\dagger h_m) m$ and an additional angular momentum quantum number \mathcal{K} associated with partial decoupling of the center-of-mass motion of an $e-h$ system in a homogeneous magnetic field.^{47,48} For a system with a finite total charge, $\mathcal{Q} = \sum_m (h_m^\dagger h_m - c_m^\dagger c_m) e \neq 0$, the partial decoupling of the center-of-mass motion means that the energy spectrum consists of degenerate LL's.⁴⁷ The states within each LL are labeled by $\mathcal{K} = 0, 1, 2, \dots$ and all have the same value of $\mathcal{L} = \mathcal{M} + \mathcal{K}$. Since both \mathcal{M} and \mathcal{K} (and hence also \mathcal{L}) commute with the PL operator \mathcal{P} , which annihilates an optically active (zero-momentum, $k = 0$) $e-h$ pair (exciton), \mathcal{M} , \mathcal{K} , and \mathcal{L} are all simultaneously conserved in the PL process.

The effects associated with finite (short) range correlations (such as formation and properties of bound states) can be studied in finite systems by exact numerical diagonalization, provided that the system size R can be made larger than the characteristic correlation length δ (i.e. the size of the bound state). Numerical diagonalization

of H for finite numbers of electrons ($N = \sum_m c_m^\dagger c_m$) and holes ($N_h = \sum_m h_m^\dagger h_m$) in a finite physical space (area) requires restriction of single-particle electron and hole Hilbert spaces to a finite size. In the planar geometry, inclusion of only a finite number of electron and hole states in the calculation (states with m only up to certain value m_{\max}) breaks the translational symmetry and the conservation of \mathcal{K} . A finite dispersion of calculated LL's, which disappears only in the $m_{\max} \rightarrow \infty$ limit, hides the underlying symmetry of the modeled (infinite) system. Also, the calculated PL oscillator strengths do not obey the exact $\Delta\mathcal{K} = 0$ optical selection rule that holds in an infinite system.

More informative finite-size spectra are obtained here using Haldane's geometry,⁴⁹ where electrons and holes are confined to a spherical surface of radius R and the radial magnetic field is produced by a Dirac monopole. The reason for choosing the spherical geometry for the calculations is strictly technical and of no physical consequence for the results. Finite area (and thus finite LL degeneracy) of a closed surface results in finite size of the many-body Hilbert spaces obtained without breaking the 2D translational symmetry of a plane (which is preserved in the form of the 2D group of rotations). The exact mapping^{34,52} between quantum numbers \mathcal{M} and \mathcal{K} on a plane and the 2D algebra of the total angular momentum \mathbf{L} on a sphere allows investigation of effects caused by those symmetries (such as LL degeneracies and optical selection rules) and conversion of the numerical results back to the planar geometry. The price paid for closing the Hilbert space without breaking the symmetries is the surface curvature which modifies the interaction matrix elements V_{ijkl}^{ee} and V_{ijkl}^{eh} . However, if the correlation length δ can be made smaller than R (as happens for both Laughlin correlations in FQH systems and for bound states), the effects of curvature are scaled by a small parameter δ/R and can be eliminated by extrapolation of the results to $R \rightarrow \infty$ (in a similar way as the results obtained in the planar geometry can be extrapolated to $m_{\max} \rightarrow \infty$).

The detailed description of the Haldane sphere model can be found for example in Refs. 49,50,53 (see also Refs. 32–34 for application to $e-h$ systems) and will not be repeated here. The strength $2S$ of the magnetic monopole is defined in the units of flux quantum $\phi_0 = hc/e$, so that $4\pi R^2 B = 2S\phi_0$ and the magnetic length is $\lambda = R/\sqrt{S}$. The single-particle states are the eigenstates of angular momentum $l \geq S$ and its projection m , and are called monopole harmonics. The single-particle energies fall into $(2l+1)$ -fold degenerate angular momentum shells (LL's). The lowest shell has $l = S$ and thus $2S$ is a measure of the system size through the LL degeneracy. The charged many-body $e-h$ states form degenerate total angular momentum (L) multiplets (LL's) of their own. The total angular momentum projection L_z labels different states of the same multiplet just as \mathcal{K} or \mathcal{M} did for different states of the same LL on a plane.

Different multiplets are labeled by L just as different LL's on a plane were labeled by \mathcal{L} . The pair of optical selection rules, $\Delta L_z = \Delta L = 0$ (equivalent to $\Delta \mathcal{M} = \Delta \mathcal{K} = 0$ on a plane) results from the fact that an optically active exciton carries no angular momentum, $l_X = 0$.

It is clear that certain properties of a “strictly” spherical system do not describe the infinite planar system that we intend to model. For example, if understood literally, finite separation d between the electron and hole spheres would lead to different values of the magnetic length in the two layers, and thus introduce an asymmetry between electron and hole orbitals (even in the lowest LL). While this effect disappears in the $R \rightarrow \infty$ limit, it is eliminated by formally calculating the matrix elements of the interaction potential $V_{eh}(r)$ at any value of d for electrons and holes confined to a sphere of the same radius R . This procedure justifies the use of spherical geometry at arbitrarily large layer separation (not only at $d \ll R$).

III. BOUND ELECTRON–HOLE STATES IN A DILUTE 2DEG

In order to understand PL from a 2DEG at arbitrary filling factor ν and layer separation d , one must first identify the bound complexes in which the holes (minority charges) can occur. After these bound complexes are found and understood in terms of such single-particle quantities as total charge \mathcal{Q} , binding energy Δ , angular momentum l , or PL oscillator strength (inverse optical lifetime) τ^{-1} , a perturbation-type analysis can be used to determine if those complexes are the relevant (or “true”) quasiparticles (TQP's) of a particular e - h system, weakly perturbed by interaction with one another and the surrounding 2DEG. If it is so, the low energy states can be understood in terms of these TQP's and their interactions. The PL (emission) probes the electron system in the vicinity of the annihilated hole and therefore the optical properties of TQP's determine the (low temperature) PL spectra of the system.

This type of analysis has been recently applied to the e - h systems at $d = 0$ in the lowest LL,^{32,33} and it showed that the low lying states contained all possible combinations of bound e - h complexes (excitons $X = e$ - h and excitonic ions $X_n^- = nX$ - e) and excess electrons, interacting through effective pseudopotentials. The short range of these pseudopotentials yields Laughlin correlations between electrons and excitonic ions, which isolate the latter from the 2DEG and make them act like well defined TQP's without internal dynamics. When applied to realistic symmetrically doped ($d = 0$) QW's at large B and low density ($\nu < \frac{1}{3}$), a similar analysis showed³⁴ that the observed PL spectra contain transitions only from radiative bound states (in that case, spin-singlet and *excited* spin-triplet X^- states) and explained why the expected³⁵ singlet-triplet X^- crossing was not observed in some experiments.¹⁴

A. Hidden Symmetry at Zero Layer Separation

The exact particle-hole symmetry between electrons and valence holes in the lowest LL at $d = 0$ results from (i) the identical electron and hole single-particle orbitals, scaled by the same characteristic length λ , which yields equal strength of e - e and e - h interaction matrix elements, $V_{ijkl}^{eh} = -V_{ikjl}^{ee}$, and (ii) no effects of different effective masses on scattering because of the infinite cyclotron gap. This “hidden symmetry” results²³ in the following commutation relation between the Hamiltonian (1) and the PL operator \mathcal{P}^\dagger which creates a $k = 0$ exciton,

$$[H, \mathcal{P}^\dagger] = E_X \mathcal{P}^\dagger, \quad (2)$$

where $E_X = -\sqrt{\pi/2} e^2/\lambda$ is the exciton energy in the lowest LL and $\mathcal{P}^\dagger = \sum_m (-1)^m c_m^\dagger h_m^\dagger$ (on the Haldane's sphere). Because of Eq. (2), a “multiplicative” (MP) eigenstate of H (a state containing N_X neutral excitons with momentum zero) can be constructed by application of \mathcal{P}^\dagger N_X times to any eigenstate of the interacting electrons. The excitons created or annihilated with operators \mathcal{P}^\dagger and \mathcal{P} (i.e. by absorption or emission of a photon) have the same energy E_X which is independent of other electrons or holes present. The number N_X of such “decoupled” excitons is conserved by H , only the states with $N_X > 0$ are radiative, and the emission (absorption) governed by the selection rule $\Delta N_X = -1$ (+1) occurs at the bare exciton energy E_X .²³

Somewhat surprisingly, it turns out^{28,30} that the “totally multiplicative” eigenstate

$$|\Psi_{N_h}\rangle = (\mathcal{P}^\dagger)^{N_h} |\Psi\rangle, \quad (3)$$

obtained by adding the Bose-condensed ground state of $N_X = N_h$ excitons each with $k = 0$ to the ground state $|\Psi\rangle$ of excess $N - N_h$ electrons, is *not always* the ground state of the combined e - h system. This results because the interaction of an excited excitonic state (i.e. one with $k \neq 0$) of the Bose condensate with the fluid of excess electrons can lower the total energy by more than the cost of creating the excited excitonic state. Typically, a MP state $\mathcal{P}^\dagger |\Phi\rangle$ created by optical injection of a $k = 0$ exciton into a state $|\Phi\rangle$ is an excited state, and the absorption is followed by relaxation to a different (non-MP, i.e. non-radiative) ground state.

The condition under which the totally MP state in Eq. (3) is the e - h ground state follows from the mapping²³ onto the $\uparrow\downarrow$ (spin-unpolarized electron) system, in which $|\Psi_{N_h}\rangle$ corresponds to the $\uparrow\downarrow$ state with the maximum spin. Since $\nu_\uparrow = 1 - \nu$ and $\nu_\downarrow = \nu_h$, and the 2DEG is spin-polarized (in the absence of the Zeeman splitting) only at the Laughlin fillings,⁵⁴ the condition for the totally MP e - h ground state $|\Psi_{N_h}\rangle$ is

$$\nu - \nu_h = 1 - (2p + 1)^{-1}, \quad (4)$$

with $p = 1, 2, \dots$. At all other fillings (e.g., $\nu - \nu_h = \frac{1}{3}$), the ground state has $N_X < N_h$, i.e. contains a number of holes that are bound in other (non-radiative) complexes than $k = 0$ excitons.

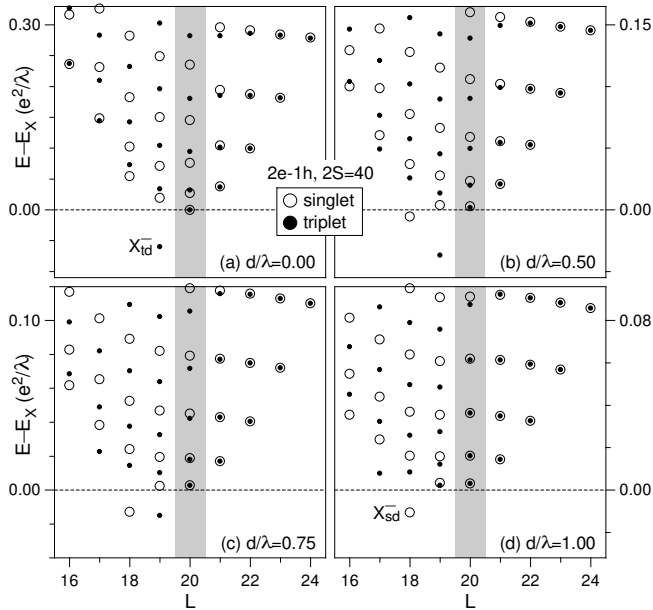


FIG. 1. The energy spectra (energy E vs. angular momentum L) of the $2e-h$ system on a Haldane sphere with the Landau level degeneracy of $2S+1 = 41$, for different values of the layer separation d . The open and full circles distinguish states with singlet and triplet electron spin configurations. E_X is the exciton energy and λ is the magnetic length.

B. Charged Exciton States

An example of a non-MP $e-h$ ground state is the “dark” spin-triplet charge exciton (X_{td}^-).³⁰ The X_{td}^- is the only bound $2e-h$ state in the lowest LL at $d = 0$. It is the most stable $e-h$ complex at $\nu_h \leq 2\nu$, but its binding energy decreases at $d > 0$ when the $e-h$ attraction (at short range) becomes smaller than the $e-e$ repulsion. The dependence of the $2e-h$ energy spectrum on d is shown in Fig. 1. The spectra are calculated in the spherical geometry for the LL degeneracy of $2S+1 = 41$. The energy is measured from the exciton energy E_X , so that for the bound states (the states below the dashed lines) it is the negative of the X^- binding energy, $\Delta_{X^-} = E_X - E$. Open and full symbols distinguish singlet and triplet electron spin configurations, and each state with $L > 0$ represents a degenerate multiplet with $|L_z| \leq L$. The Zeeman energy of the singlet states is not included. The angular momentum L calculated on a sphere translates into the angular momentum quantum numbers on a plane in such way^{34,52} that each LL at $\mathcal{L} = 0, -1, -2, \dots$ (containing states with $\mathcal{K} = 0, 1, 2, \dots$, i.e. with $\mathcal{M} = \mathcal{L} - \mathcal{K} = \mathcal{L}, \mathcal{L} - 1, \mathcal{L} - 2, \dots$) is represented by a multiplet at $L = S + \mathcal{L}$. Thus, the low energy multiplets in Fig. 1 at $L = 20, 19$, and 18 represent the planar LL’s at $\mathcal{M} \leq \mathcal{L} = 0$, $\mathcal{M} \leq \mathcal{L} = -1$, and $\mathcal{M} \leq \mathcal{L} = -2$, respectively.

It is important to realize that the recombination of an isolated X_{td}^- at $d = 0$ is forbidden because of two independent symmetries.^{32–34} The $\Delta N_X = -1$ selection rule

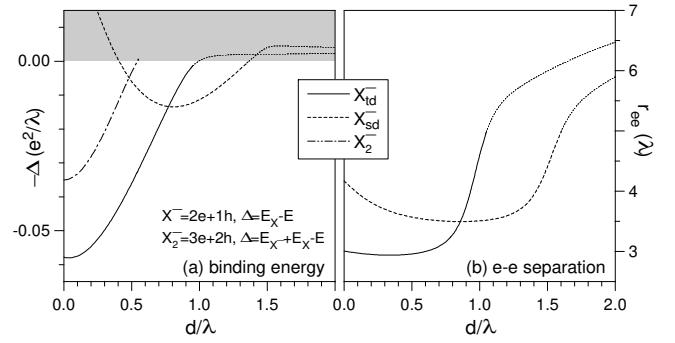


FIG. 2. The binding energy Δ of the triplet and singlet charged exciton states, X_{td}^- and X_{sd}^- , and of the charged biexciton, X_2^- , as a function of layer separation d . E_X is the exciton energy and λ is the magnetic length.

resulting from the hidden symmetry, which allows recombination from a pair of MP states at $L = S$ and $E = E_X$ only, is lifted at $d > 0$. However, the translational symmetry yielding conservation of L and L_z (on a plane, \mathcal{M} and \mathcal{K}) holds at any value of d . Because the electron left in the lowest LL after recombination has $l = S$ ($\mathcal{L} = 0$), only those $2e-h$ multiplets at $L = S$ ($\mathcal{L} = 0$) are radiative. They are marked with shaded rectangles in all frames of Fig. 1. In larger systems containing more than a single X^- , the translational symmetry is broken by collisions, and weak X_{td}^- recombination becomes possible.

The X_{td}^- binding energy $\Delta_{X_{td}^-}$, calculated by extrapolation of data obtained for $2S \leq 60$, is about $0.052 e^2/\lambda$ at $d = 0$ (very close to the value obtained earlier by Palacios et al.³¹ in the planar geometry). As expected, $\Delta_{X_{td}^-}$ decreases with increasing separation up to $d \approx \lambda$, when X_{td}^- unbinds. Somewhat surprisingly, a new bound multiplet, a singlet X_{sd}^- at $L = S - 2$ ($\mathcal{L} = -2$), occurs at finite d . Its binding $\Delta_{X_{sd}^-}$ reaches maximum of about $0.013 e^2/\lambda$ at $d \approx 0.8\lambda$. The X_{sd}^- is a non-radiative (“dark”) state and should be distinguished from the radiative singlet state X_s^- at $L = S$ ($\mathcal{L} = 0$), which is the X^- ground state at low magnetic fields (and small d). The X_{sd}^- is a $2e-h$ analog of the singlet D^- state (two electrons bound to a distant donor impurity) with the same $\mathcal{L} = -2$. A series of transitions between singlet and triplet D^- states with increasing $|\mathcal{L}|$ have been found when the distance between the impurity and the electron layer were increased.⁴²

Bound states of larger excitonic ions $X_n^- = nX + e$ are also possible at small d . They all have completely polarized electron and hole spins, and their binding energy, $\Delta_{X_n^-} = E_X + E_{X_{n-1}^-} - E$, decreases with increasing size (n). The dependence of X_{td}^- , X_{sd}^- , and X_2^- binding energies (calculated at $2S = 60$) on separation d is shown in Fig. 2(a). As it was discussed in Sec. II, finite-size calculations give good approximation to $2e-h$ energies only for the bound (finite-size) states. While the binding energies are correct at the values of d for which $\Delta > 0$, they should asymptotically approach zero for $d \rightarrow \infty$ instead of crossing it as in Fig. 2(a). The average $e-e$ distance

$r_{ee} = \sqrt{\langle r_{ee}^2 \rangle}$ within the X_{td}^- and X_{sd}^- complexes is plotted in Fig. 2(b). Both X^- wavefunctions depend rather weakly on d in the range where $\Delta > 0$ (i.e., $d \leq 0.7\lambda$ for X_{td}^- and $0.4\lambda \leq d \leq 1.2\lambda$ for X_{sd}^-), but when d exceeds the critical value ($d = 0.8\lambda$ for X_{td}^- and $d = 1.3\lambda$ for X_{sd}^-), r_{ee} quickly increases and the X^- unbinds into an exciton and an electron. Similarly as for binding energies in Fig. 2(a), we expect the r_{ee} curves in Fig. 2(b) to correctly describe the X_{td}^- and X_{sd}^- states on an infinite plane only when r_{ee} is smaller than $R \approx 5\lambda$.

IV. ELECTRON-HOLE STATES AT SMALL LAYER SEPARATION: ELECTRON-CHARGED-EXCITON FLUID

A. Zero Layer Separation

In the following the 2DEG is assumed to be completely spin-polarized because of large Zeeman splitting. We do not discuss effects due to X_{sd}^- and omit the spin subscript in the triplet charged-exciton state X_{td}^- . It follows from Figs. 1 and 2 that X^- is the only spin-polarized bound $2e-h$ state at $d \leq \lambda$. Since $\Delta_{X^-} > \Delta_{X_2^-} > \Delta_{X_3^-} > \dots$ in entire range of d , the excitonic ions larger than X^- are unstable in the presence of excess electrons (e.g., $X_2^- + e \rightarrow 2X^-$), and the low lying states at $d < \lambda$ and $\nu_h \ll \nu$ contain only X^- 's and electrons interacting with one another through effective pseudopotentials.^{32,33} The pseudopotential $V_{eX^-}(L)$ (the $e-X^-$ pair interaction energy V as a function of pair angular momentum L) at $d = 0$ was shown³³ to satisfy the ‘‘short range’’ criterion⁴⁵ at those values of L which correspond to odd ‘‘relative’’ pair angular momenta $\mathcal{R} = l_e + l_{X^-} - L$ (\mathcal{R} is equal to the usual relative pair angular momentum m on a plane). As a result, generalized Laughlin correlations described in the wavefunction by a Jastrow prefactor $\prod_{ij} (z_e^{(i)} - z_{X^-}^{(j)})^{m_{eX^-}}$ with even exponents m_{eX^-} occur in the two-component $e-X^-$ fluid. At certain values of the electron and hole filling factor, these correlations result in incompressibility. For example, the $[m_{ee}m_{X^-X^-}m_{eX^-}] = [332]$ ground state, first suggested by Halperin⁴³ for the $\uparrow\downarrow$ spin fluid, has been found numerically in the $8e-2h$ system.³³ A generalized (multi-component) mean-field composite fermion (CF) model has been proposed³³ to determine the bands of lowest energy states at any ν and ν_h . In this model, effective CF magnetic fields of different type (color) result which cannot be understood literally. Rather, the model relies on two simple facts:^{33,45} (i) in the low energy states of Laughlin-correlated many-body systems, a number of strongly repulsive pair states at the smallest \mathcal{R} are avoided for each type of pair (here, $e-e$ and $e-X^-$); (ii) the states satisfying the above constraint can be found more easily by noticing that the avoiding of pair states with the smallest \mathcal{R} is equivalent to the binding of zeros of the many-body wavefunction (vortices), which can

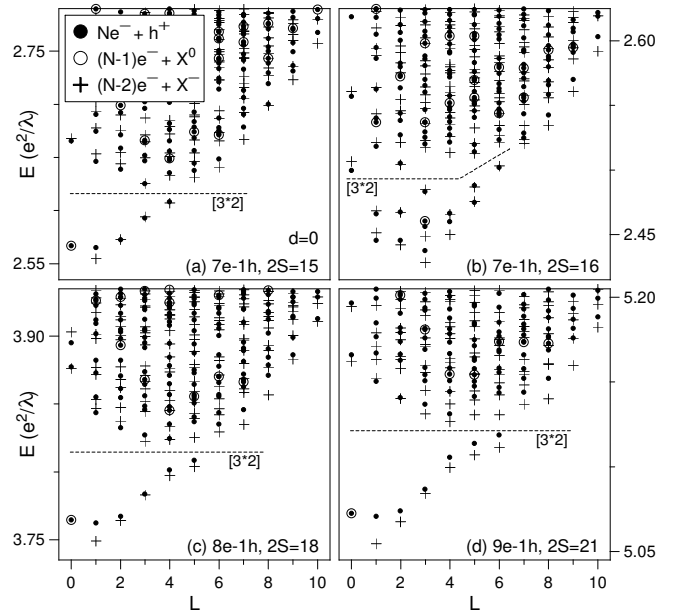


FIG. 3. The energy spectra (energy E vs. angular momentum L) of the co-planar ($d = 0$) $Ne-h$ systems on a Haldane sphere with the Landau level degeneracy of $2S + 1$: (a) $N = 7$ and $2S = 15$, (b) $N = 7$ and $2S = 16$, (c) $N = 8$ and $2S = 18$, and (d) $N = 9$ and $2S = 21$. Full dots: exact $Ne-h$ spectra; open circles: multiplicative states; pluses: approximate energies of $(N - 2)e-X^-$ states. The non-multiplicative states below the dashed lines are $(N - 2)e-X^-$ states with Laughlin-Halperin $[3^*2]$ correlations. λ is the magnetic length.

be reproduced (for the purpose of multiplet counting) by attachment of magnetic fluxes.

Let us apply the CF model to the system containing N electrons and only one hole. While the correct picture of this simple system is essential for understanding the nature of low energy states and (low-temperature) PL of a 2DEG in the FQH regime, it has been interpreted incorrectly in a number of previous studies.²⁷ In Fig. 3 we show the energy spectra for $N = 7, 8$, and 9 and $2S$ corresponding to $\nu \approx \frac{1}{3}$. The full dots mark the multiplets obtained in the exact diagonalization of the $Ne-h$ system and the open circles mark the MP states (with an $l_{X^-} = 0$ exciton decoupled from the $N - 1$ electron fluid).

In Fig. 3(acd), the $N - 1$ electrons in the lowest energy MP state at $L = 0$ form the Laughlin $\nu = \frac{1}{3}$ ground state. In Fig. 3(b), there is one Laughlin quasihole in the lowest MP state at $L = 3$. The non-MP low energy states in all frames contain an X^- with angular momentum $l_{X^-} = S - 1$ and $N - 2$ electrons each with $l_e = S$. The CF picture in which two magnetic fluxes are attached to each particle to model the avoiding of the $\mathcal{R}_{ee} \leq 2$ and $\mathcal{R}_{eX^-} \leq 1$ pair states yields effective angular momenta of $l_e^* = l_e - (N - 2)$ and $l_{X^-}^* = l_{X^-} - 1$. In Fig. 3(acd) the $N - 2$ electrons leave one Laughlin quasihole (QH_e) with angular momentum $l_{QH_e} = l_e^*$ in their $(2l_e^* + 1)$ -fold degenerate CF level, and the X^- becomes a single Laughlin ‘‘quasielectron’’ (QE_{X^-}) with $l_{QE_{X^-}} = l_{X^-}^*$. The allowed

angular momenta L of the $\text{QH}_e\text{-QE}_{X^-}$ pair in the lowest energy states of these $(N-2)e\text{-}X^-$ systems are obtained by adding l_{QE_e} and $l_{\text{QE}_{X^-}}$ of two distinguishable particles. The result is: $L = 1, 2, \dots, N-3$. Indeed, the multiplets at these values of L form the lowest band of non-MP states in Fig. 3(acd), separated from higher states by dashed lines. The dependence of energy on L within these bands can be interpreted as the $\text{QH}_e\text{-QE}_{X^-}$ pseudopotential, and its increase with L means that it is attractive (for a pair of opposite charges, L increases with increasing average separation). The $L = 1$ ground states in Fig. 3(acd) should be therefore understood as an excitonic bound states of a $\text{QH}_e\text{-QE}_{X^-}$ pair in the Laughlin $e\text{-}X^-$ fluid. In this state, a Laughlin QH type excitation of charge $+\frac{1}{3}e$ is bound to the X^- , and the total charge of the X^- -QH state is $\mathcal{Q} = -\frac{2}{3}$. A similar analysis for Fig. 3(b) gives $l_e^* = 3$ and $l_{X^-}^* = 2$, yielding two QH_e 's each with $l_{\text{QH}_e} = 3$ and one QE_{X^-} with $l_{\text{QE}_{X^-}} = 2$. The allowed values of L for such three particles are: $1^2, 2^2, 3^3, 4^2, 5^2, 6$, and 7 , exactly as found for the lowest non-MP states in Fig. 3(b).

The strongest indication that the lowest energy bands of non-MP states in Fig. 3 contain an X^- interacting with excess electrons comes from direct comparison of exact $Ne\text{-}h$ energies (dots) with the approximate energies of the $(N-2)e\text{-}X^-$ charge configuration (pluses). The $(N-2)e\text{-}X^-$ energies are calculated using an effective $e\text{-}X^-$ pseudopotential and the X^- binding energy. Since the results depend on unknown details of V_{eX^-} (due to the density-dependent polarization of the X^- in the electric field of electrons), we make a (rough) approximation and instead of V_{eX^-} use the pseudopotential of two distinguishable point charges with angular momenta l_e and l_{X^-} . The obtained spectra are quite close to the original ones and all contain the low lying bands as predicted by the CF model. A much better fit is obtained for V_{eX^-} including (N -dependent) polarization effects.

It is apparent that only two types of states exhaust the entire low energy spectra shown in Fig. 3: the MP states containing a decoupled $l_X = 0$ exciton and the non-MP states containing an X^- . None of the low energy states can be understood in terms of an excited ($l_X \neq 0$) exciton interacting with the excess $N-1$ electrons. In particular, the bands of lowest energy states at $L = 1, 2, \dots, N-3$ in Fig. 3(acd) do not describe dispersion of a so-called ‘‘dressed exciton’’ X^* (charge neutral exciton with an enhanced mass due to the coupling to $\text{QE}\text{-QH}$ pair excitations of the Laughlin $\nu = \frac{1}{3}$ fluid of $N-1$ excess electrons) as first suggested by Apalkov and Rashba²⁶ and reviewed in subsequent papers. It is much more informative to interpret these $e\text{-}h$ states in terms of a well defined X^- particle (with specified $\mathcal{Q} = -e, l = S-1$ or $\mathcal{L} = -1, \Delta$ as plotted in Fig. 2, and $\tau^{-1} = 0$) interacting with excess electrons through the well defined^{32,33} pseudopotential V_{eX^-} yielding well defined Laughlin-Jastrow $e\text{-}X^-$ correlations and Laughlin quasiparticle excitations of a two-component incompressible ‘‘reference’’ state, than to

say that $k \neq 0$ exciton is coupled in an undefined way to the Laughlin quasiparticles of an electron $\nu = \frac{1}{3}$ state. The ‘‘dressed exciton’’ picture is simply wrong in describing the nature of the TQP of the system. For example, the X^* has zero charge and continuous energy spectrum instead of $\mathcal{Q} = -e$ and Landau quantized orbits of an X^- . The reason why the suggestive idea of an X^* does not work is that the coupling of a $k \neq 0$ exciton (which has a nonzero in-plane electric dipole moment $\mu \propto k$) to electrons is too strong to be treated perturbatively.

B. Small Layer Separation

The knowledge of the nature of the TQP's of any system is essential for understanding its response to an external perturbation. Since an X^* is expected to behave differently than an X^- when electron and hole layers are separated, the incorrect assumption of the ‘‘dressed exciton’’ picture at $d = 0$ must result in incorrect interpretation of the $e\text{-}h$ states at $d > 0$ as well.

At a small layer separation $d < \lambda$, all bound $e\text{-}h$ states acquire a small electric dipole moment μ , which is proportional to d and oriented perpendicular the electron and hole planes. These dipole moments result in a repulsive dipole-dipole interaction between $e\text{-}h$ complexes, which is proportional to d^2/r^3 at distance $r \gg d$. While the electron-dipole $e\text{-}X$ repulsion is the reason for the decrease of the binding energy of an isolated X^- at $0 < d \ll \lambda$, it can slightly extend the stability range of an X^- embedded in a 2DEG (compared to Fig. 2).

In the range of d values for which the X^- is bound, the X^- dipole moment increases its total repulsion with electrons and other X^- 's. It is possible that this increased repulsion could enhance the excitation gap of an incompressible fluid $e\text{-}X^-$ state. Examples of different behavior of the gap are shown in Fig. 4. In Fig. 4(a), the $9e\text{-}h$ ground state at $d = 0.5\lambda$ is the $7e\text{-}X^-$ state with $[3^*2]$ correlations ($m_{X^-X^-}$ is undefined for only one X^-). In the generalized CF picture, this state contains one QE_{X^-} with $l_{\text{QE}} = 2$ and a filled shell of electron CF's. In Fig. 4(b), the $8e\text{-}2h$ ground state at $d = 0.5\lambda$ is the $4e\text{-}2X^-$ incompressible state $[332]$. In Fig. 4(c), the $6e\text{-}3h$ ground state at $d = 0.3\lambda$ is the Laughlin $\nu = \frac{1}{5}$ state of three X^- 's (here, pluses mark approximate $3X^-$ energies obtained by diagonalizing a system of three fermions each with energy E_{X^-} and interacting through $V_{X^-X^-}$). As shown in Fig. 4(d), the excitation gaps of these three different Laughlin-correlated ground states behave differently as a function of d . In particular, the gap of the $\nu = \frac{1}{5}$ state of X^- 's increases significantly up to $d = 0.7\lambda$.

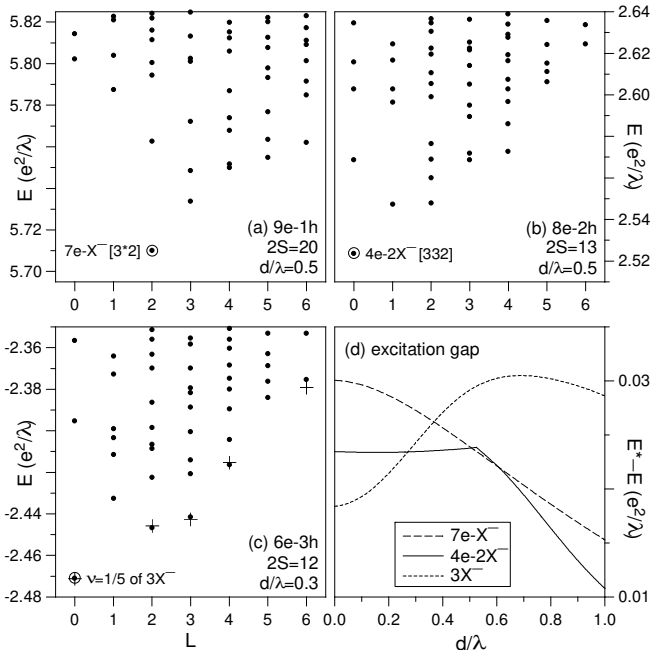


FIG. 4. (abc) The energy spectra (energy E as a function of angular momentum L) of electron-hole systems with Laughlin $e-X^-$ correlations in a $9e-h$ system at the layer separation $d = 0.5\lambda$; (b) $4e-2X^-$ incompressible ground state [332] in a $8e-2h$ system at $d = 0.5\lambda$; (c) Laughlin $\nu = \frac{1}{5}$ ground state of three X^- 's in a $6e-3h$ system at $d = 0.3\lambda$ (pluses show approximate $3X^-$ energies). (d) The excitation gaps of ground states in frames (abc) as a function of d . λ is the magnetic length.

V. ELECTRON-HOLE STATES AT LARGE LAYER SEPARATION: HOLE WEAKLY COUPLED TO ELECTRON FLUID

It was shown by Chen and Quinn²⁸ that the opposite limit of $d \gg \lambda$ is easier to understand than that of $d < \lambda$, because of the vanishing $e-h$ interaction. In this limit, the low lying states of the combined system are products of the Laughlin-correlated 2DEG and the decoupled hole. The allowed angular momenta L of the lowest energy band of the combined $e-h$ system result from addition of the angular momenta of the lowest energy electron states (containing a number of Laughlin quasiparticles) L_e to the hole angular momentum $l_h = S$.

A decrease of d to a few magnetic lengths λ does not yet result in exciton binding because the length scale D probed by the potential of a distant hole exceeds the average $e-e$ separation in the 2DEG. While the $e-e$ interactions alone still completely determine the (Laughlin) correlations of the 2DEG, the valence band hole can now correlate with the quasiparticle excitations of the 2DEG due to their much lower density (compared to the electron density). The hole repels positively charged QH's but can bind one or more negatively charged QE's (depending on the relative strength of the $h-QE$ and $QE-QE$ in-

teractions) to form fractionally charged excitons (FCX), or “anyonic ions,” hQE_n .²⁸ When d is so large that the number of Laughlin quasiparticles in the 2DEG is conserved by the weak $e-h$ interaction, a discontinuity in the behavior of the system as a function of the magnetic field (or electron density) will occur at Laughlin filling factors $(2p+1)^{-1}$, because different type of TQP's can form depending on whether QE's are or are not present in the 2DEG. The transition should be visible in PL, as the recombination of a free hole at $\nu < (2p+1)^{-1}$ can be distinguished from that of a hole bound into an hQE_n complex at $\nu > (2p+1)^{-1}$.

VI. ELECTRON-HOLE STATES AT INTERMEDIATE LAYER SEPARATION

The TQP's of the $e-h$ system at a particular layer separation d are by definition the most stable bound complexes (the ones with the largest binding energy) composed of smaller elementary particles or quasiparticles: a valence hole and either electrons or Laughlin excitations of the 2DEG. To determine the most stable complexes at a particular value of d , the interactions between their sub-components must be studied. Two-body interactions enter the many-body Hamiltonian through their pseudopotentials $V(L)$, defined as the pair interaction energy V as a function of pair angular momentum L (or another pair quantum number).^{44,45} The $e-e$, $e-h$, $QE-QE$, $QH-QH$, and $QE-QH$ pseudopotentials are well-known^{44,45,55} and (except for $e-h$) do not depend on d for spatially separated electron and hole layers. The simple form of single-particle wavefunctions in the lowest LL results in very regular form of $V_{ee}(L)$ and $V_{eh}(L)$. On a sphere, larger L corresponds to smaller (larger) average separation of two charges of the same (opposite) sign, and thus V_{ee} increases and $|V_{eh}|$ decreases with increasing L .

The dependence of $V_{eh}(L)$ on d can be expressed in terms of the effective strength (U) and range (D) of the Coulomb potential of the hole (in its lowest-LL single-particle state) seen by an electron. A measure of U is the exciton binding energy $\Delta_X = V_{eh}(0)$. As shown in Fig. 5(a), Δ_X varies with d roughly as $\Delta_X(d) = (1+d/\lambda)^{-1}\Delta_X(0)$, which means that the average $e-h$ separation in the exciton ground state is roughly $r_{eh}(d) = r_{eh}(0) + d$ rather than $\sqrt{r_{eh}^2(0) + d^2}$. A measure of the range D is an average $e-h$ distance r_{eh} in the exciton state whose energy is half of the binding energy. In Fig. 5(b) we plot the normalized exciton pseudopotentials as a function of wavevector $k = L/R$. Since r_{eh} is proportional⁵⁶ to k , and the value $k_{1/2}$ for which $V_{eh}(k_{1/2}) = -\frac{1}{2}\Delta_X$ in Fig. 5(b) increases roughly linearly with d , we obtain the pair of relations,

$$\begin{aligned} U &\propto (1+d/\lambda)^{-1}, \\ D &\propto d/\lambda, \end{aligned} \quad (5)$$

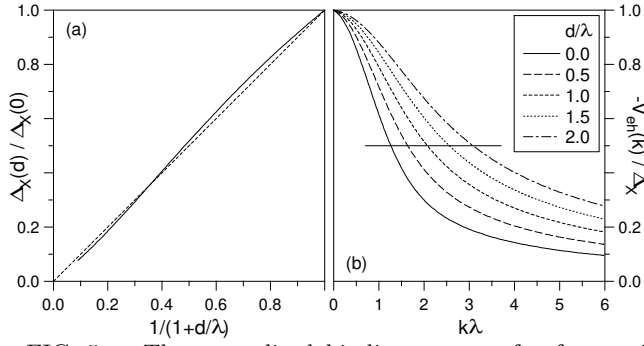


FIG. 5. The normalized binding energy of a free excitation, $\Delta_X(d)/\Delta_X(0)$, as a function of $(1+d/\lambda)^{-1}$ (a), and the normalized electron-hole pseudopotentials $V_{eh}(k)/(-\Delta_X)$ as a function of wavevector k (b). d is the separation between electron and hole layers, and λ is the magnetic length.

describing the perturbing potentials V_{UD} which can be achieved in bi-layer e - h systems with different d .

Laughlin quasiparticles have more complicated charge density profiles than electrons or holes in the lowest LL. This internal structure is reflected in the oscillations of the QE and QH pseudopotentials at the values of L corresponding to small average separation between the QE or QH and the second particle. For example, despite Laughlin quasiparticles being charge excitations, neither QE-QE nor QH-QH interaction is generally repulsive.^{55,57} On the contrary, the QE₂ molecule (the state with maximum L , i.e. minimum average QE-QE separation) is either the ground state or a very weakly excited state of two QE's (the numerical results for finite systems are not conclusive).⁵⁵

In order to calculate the pseudopotentials $V_{hQE}(L)$ and $V_{hQH}(L)$ associated with the interaction between Laughlin quasiparticles (QE or QH) of a $\nu = \frac{1}{3}$ fluid and a hole moving in a parallel plane separated by an arbitrary distance d , we use the following procedure. A finite Ne - h system is diagonalized at the monopole strength $2S$ corresponding to a single QE or QH in the 2DEG (in the absence of the interaction with the hole). To assure that the interaction between the hole and the 2DEG is weak compared to the energy $\epsilon_{QE} + \epsilon_{QH}$ ($\approx 0.1 e^2/\lambda$ for an infinite system) needed to create additional QE-QH pairs in the 2DEG, the charge of the hole is set to e/ϵ where $\epsilon \gg 1$. This guarantees that the lowest band of Ne - h states contain exactly one QE or QH interacting with the hole. The pseudopotentials $V_{hQE}(L)$ and $V_{hQH}(L)$ are calculated by subtracting from the lowest eigenenergies the constant energy of the 2DEG and the energy of interaction between the hole and the uniform-density $\nu = \frac{1}{3}$ fluid, and multiplying the difference by ϵ . If ϵ is sufficiently large, the pseudopotentials calculated in this way (and shown in Fig. 6(ab)) do not depend on ϵ and describe the interaction between the hole of full charge $+e$ and the Laughlin quasiparticle.

A similar procedure has been used to calculate the pseudopotentials $V_{eQH}(L)$ and $V_{eQE}(L)$ of the interaction

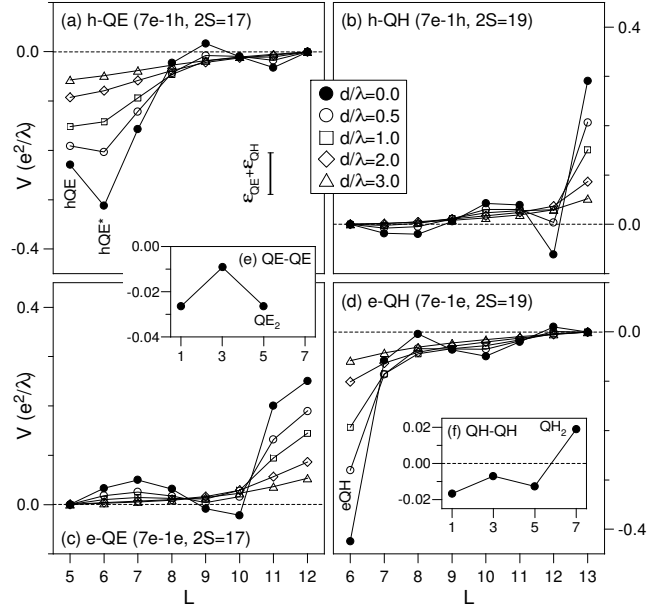


FIG. 6. The pseudopotentials (pair energy V as a function of pair angular momentum L) of the interaction between quasiparticles (quasielectron QE and quasihole QH) of the seven-electron Laughlin $\nu = \frac{1}{3}$ state and an additional charge (electron or hole) on a parallel layer separated by d . The QE-QE and QH-QH pseudopotentials for $N = 7$ are shown in inset frames (ef). ϵ_{QE} and ϵ_{QH} are the QE and QH energies and λ is the magnetic length.

between quasiparticles and an electron moving in a parallel layer [Fig. 6(cd)], and the pseudopotentials $V_{hQE_n}(L)$ and $V_{eQE_n}(L)$ involving the QE₂ and QE₃ molecules (Fig. 7). From such calculation, the binding energies and PL oscillator strengths of all hQE_n FCX's are obtained to determine under what circumstances (layer separation, density, temperature, etc.) various FCX's can occur and contribute to the PL spectrum.

The pseudopotentials of a single QE and QH of a seven-electron fluid ($N = 7$) interacting with a hole or an electron on a parallel layer are shown in Fig. 6(ab) for a number of different layer separations d . The allowed pair angular momenta L result from addition of individual angular momenta of the quasiparticles,⁵⁵ $l_{QE} = l_{QH} = N/2$, and the particles in the second layer, $l_e = l_h = S$. Since the length scale D probed by the potential of the hole (electron) decreases when it is brought closer to the 2DEG, structure appears for $d < \lambda$ in all pseudopotentials (at L corresponding to small average separation). For example, the h -QE ground state for $d < \lambda$ occurs at $L > l_h - l_{QE}$, i.e. not at the minimum allowed average h -QE separation. Similarly as in QE-QE and QH-QH pseudopotentials⁵⁵ (see also Fig. 6(f) for $N = 7$), the oscillations of particle-quasiparticle pseudopotentials reflects structure in QE and QH charge density.

All pseudopotentials in Figs. 6 and 7 have been arbitrarily shifted in energy so that they vanish for the pair state of the largest average separation. The more accu-

rate estimate of the h -QE pseudopotential parameters at the two smallest values of L , i.e. the binding energy Δ of the h QE and h QE* complexes with the smallest and the next smallest average h -QE separation (the h QE* complex is important in discussion⁴⁶ of PL) gives the curves plotted in Fig. 8. The interaction of the 2DEG at $\nu \approx \frac{1}{3}$ with an additional charge (hole or electron) can be considered weak only at about $d > 1.5\lambda$. In this regime, the 2DEG responds to the perturbation introduced by a distant charge by screening it with already existing Laughlin quasiparticles to form bound FCX's, h QE or e QH. A discontinuity occurs at $\nu = \frac{1}{3}$, because the QE's that can be bound to a hole exist only at $\nu > \frac{1}{3}$, and the QH's that can be bound to an electron occur only at $\nu < \frac{1}{3}$. Fig. 8 shows that at $d < 1.5\lambda$ the energy of h -QE (and e -QH) attraction exceeds $\varepsilon_{\text{QE}} + \varepsilon_{\text{QH}}$ and the QE-QH pairs are spontaneously created in the 2DEG to screen the hole (or electron) charge at any value of $\nu \approx \frac{1}{3}$.

Whether only one QE-QH pair will be spontaneously created to form h QE, or if additional QE-QH pairs will be created to form larger FCX's (e.g., h QE \rightarrow h QE₂+QH) depends on $V_{h\text{QE}_2}$ and $V_{h\text{QE}_3}$. Since $V_{\text{QE-QE}}$ has a minimum at $L = 2l_{\text{QE}} - 1$ ($\mathcal{R} = 1$) and a maximum at $L = 2l_{\text{QE}} - 3$ ($\mathcal{R} = 3$), two or three QE's can form QE₂ or QE₃ molecules. Even if the QE₂ and QE₃ molecules do not turn out to be the absolute two- or three-QE ground states in the absence of an additional attractive potential, they both will be metastable due to the energy barrier at $\mathcal{R} = 3$, i.e. a finite energy gap to separate two QE's. Both QE₂ and QE₃ can bind to a hole, and (because of the barrier in $V_{\text{QE-QE}}$) the resulting FCX's, h QE₂ and h QE₃, could be expected to be quite stable even at $d \gg \lambda$.

The pseudopotentials describing interaction of the QE₂ and QE₃ molecules with a hole and an electron are shown in Fig. 7. Somewhat unexpectedly, they show that QE₂ is more strongly attracted to the hole than QE₃, which suggests that the h QE₃ is not stable (h QE₃ \rightarrow h QE₂+QE). Since the h -QE₂ attraction is also stronger than h -QE in Fig. 6, both h QE and h QE₂ are stable FCX's.

The binding energies Δ of all h QE _{n} complexes calculated in the $8e$ - h system are plotted as a function of d in Fig. 8. The binding energy Δ of an h QE _{n} state is defined as the energy of attraction between the hole and n QE's. For the excitonic state he (in which a hole binds a whole "real" electron to form an e - h pair weakly coupled to the remaining $N - 1$ electrons at $2S = 3(N - 2)$, i.e. at $\nu = \frac{1}{3}$) with energy E_{he} , Δ_{he} is defined as a difference between E_{he} and the state in which the hole is completely decoupled from all N electrons (which at $2S = 3(N - 2)$ form a state with three Laughlin QE's). Note that Δ_{he} is not equivalent to the binding energy of a free exciton (it is not equal to the e - h attraction but also includes the energy needed to remove an electron from the Laughlin state so that it can be bound to the hole).

The h QE₂ is the most strongly bound FCX in entire range of d (at least up to $d = 10\lambda$), and hence it is

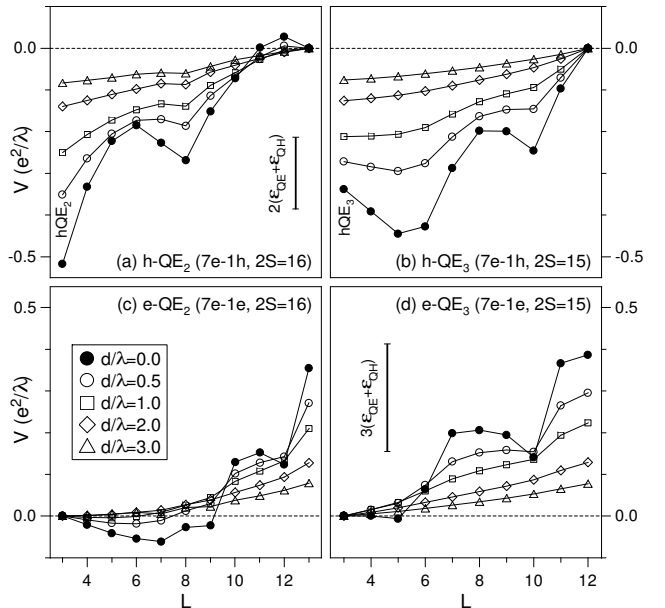


FIG. 7. The pseudopotentials (pair energy V versus pair angular momentum L) of the interaction between molecules consisting of two or three quasielectrons (QE₂ and QE₃) of the Laughlin $\nu = \frac{1}{3}$ state and an additional charge (electron or hole) on a parallel layer separated by d . ε_{QE} and ε_{QH} are the QE and QH energies and λ is the magnetic length.

expected to form in the presence of excess QE's at $\nu > \frac{1}{3}$. It can be seen in Fig. 8 that $\Delta_{h\text{QE}_2} > \varepsilon_{\text{QE}} + \varepsilon_{\text{QH}}$ at $d < \lambda$, and two QE-QH pairs are spontaneously created in the 2DEG to form h QE₂ even at $\nu < \frac{1}{3}$. However, at such small d , neutral (X) and charged excitons (X^-) composed of a hole and one or two "real" electrons of charge $-e$ (rather than Laughlin QE's of charge $-\frac{1}{3}e$) are more stable complexes than h QE₂. The transition from fractional to "normal" exciton phase occurs at $d \approx 1.5\lambda$, that is at the crossing of $\Delta_{h\text{QE}_2}$ and Δ_{he} in Fig. 8 (the shaded rectangle marks the "normal" exciton phase).

VII. NUMERICAL ENERGY SPECTRA

Using a modified Lanczos algorithm, we have been able to quickly and exactly diagonalize Hamiltonians of dimensions up to $\sim 10^6$. This allowed calculation of energy and PL spectra of N e - h systems with $N \leq 9$ and at the values of $2S$ up to $3(N - 1)$, corresponding to the hole interacting with the Laughlin $\nu = \frac{1}{3}$ state of N electrons. The $9e$ - h energy spectra (energy E as a function of angular momentum L) obtained for different values of $2S$ and d have been shown in Figs. 9–13. In all figures, the open circles at $d = 0$ mark the MP states, in which a $k = 0$ exciton is decoupled from remaining electrons.

$2S = 20$ (Fig. 9): The spectrum for $d = 0.5\lambda$ has already been shown in Fig. 4(a). At a low layer separation ($d \leq \lambda$), the ground state at $L = 2$ is the $7e$ - X^- Laughlin-correlated state [3^*2]. In the CF picture of this

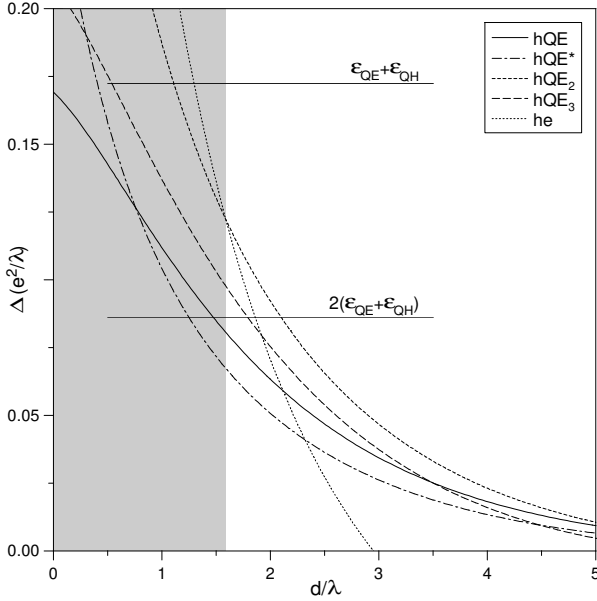


FIG. 8. The binding energy Δ of fractionally charged excitons hQE_n as a function of layer separation d , calculated for the $8e-h$ system with a fixed number of Laughlin quasiparticles in the $8e$ electron system ($\epsilon \gg 1$; see text). λ is the magnetic length. The he state contains an exciton and originates from the multiplicative state at $d = 0$. In the shaded part of the graph, the he has the largest binding energy and the hQE_n complexes do not form.

state, seven electrons fill completely their CF shell of $l_e^* = S - (N - 2) = 3$ and the X^- becomes a “quasielectron” (QE_{X^-}) with $l_{X^-}^* = l_e^* - 1 = 2$.

At $d \approx 2\lambda$, the X^- unbinds and the $7e-X^-$ fluid undergoes reconstruction. Since four QE’s of the nine electron Laughlin $\nu = \frac{1}{3}$ state cannot all bind to the hole, the ground state at the intermediate separations ($1.5\lambda \leq d \leq 4\lambda$) does not correspond to a single bound FCX. Instead, the low lying states describe different unbound states of the hole and four QE’s which occur in this particular finite-size system (but have no significance in an infinite system).

At very large separations ($d > 4\lambda$) the spectrum simplifies due to the weakening of h -QE interactions, and well defined bands develop in the low energy spectrum. In these bands, the hole with angular momentum $l_h = S = 10$ is weakly coupled to different states of four QE’s in Laughlin fluid of nine electrons. Each QE has $l_{QE} = S - (N - 1) + 1 = 3$, the allowed total angular momenta of four QE’s are $L_{4QE} = 0, 2, 3, 4$, and the h -4QE bands start at $L = |l_h - L_{4QE}| = 10, 8, 7, 6$, and 4. All these bands (except for the band with $L_{4QE} = 0$ and $L = 10$ which has too high energy at $d \leq 4\lambda$) are marked in Fig. 9(e) with solid lines. The states within each h -4QE band become degenerate at $d/\lambda \rightarrow \infty$.

$2S = 21$ (Fig. 10): The spectrum for $d = 0$ has already been shown in Fig. 3(d). As explained in Sec. IV A, the lowest energy state at $L = 0$ is the MP state, and the

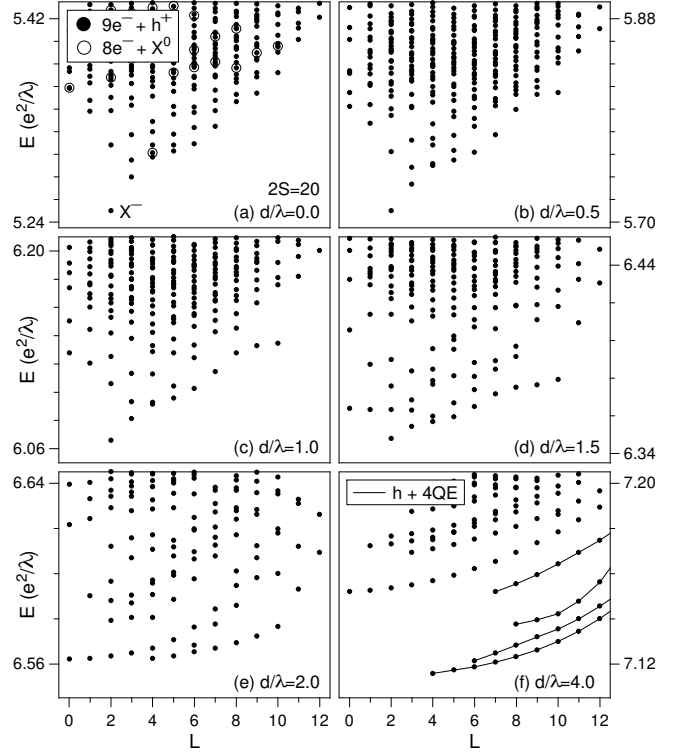


FIG. 9. The energy spectra (energy E vs. angular momentum L) of the $9e-h$ system calculated on a Haldane sphere with monopole strength $2S = 20$ for different layer separations d . The open circles mark the multiplicative states at $d = 0$. λ is the magnetic length.

band of states connected with solid lines describe excitonic spectrum of an X^- interacting with one QH of the two-component Laughlin $[3^*2]$ state of the $7e-X^-$ fluid. Clearly, this band survives also in the spectra at $d > 0$. The X^- -QH states at the largest E and L (in which the X^- is far away from the QH) gain energy and fall into the continuum at $d \approx \lambda$, i.e. when the X^- is expected to unbind. In the X^- -QH state at $L = 1$, the positively charged QH is closely bound to the X^- which reduces its total charge (the total charge of the X^- -QH is $Q = -\frac{2}{3}$, compared to $Q = -1$ for a free X^-), and stabilizes the X^- -QH state up to at least $d = 2\lambda$.

The band of states marked with dashed lines contains the hQE_2 (most stable of all FCX’s) interacting with the third QE (note that here QE denotes quasielectron of the Laughlin $\nu = \frac{1}{3}$ state of nine electrons, not of the two-component $7e-X^-$ state $[3^*2]$). The allowed angular momenta of the hQE_2 -QE pair can be obtained by adding two $l_{QE} \equiv S - (N - 1) + 1 = \frac{7}{2}$ to obtain $l_{QE_2} \equiv 2l_{QE} - 1 = 6$ and then adding to it $l_h = \frac{21}{2}$ to obtain $l_{hQE_2} \equiv |l_h - l_{QE}| = \frac{9}{2}$. Finally, adding l_{hQE_2} to l_{QE} as if they were completely distinguishable particles gives $|l_{hQE_2} - l_{QE}| \leq L \leq l_{hQE_2} + l_{QE}$, or $1 \leq L \leq 8$. However, because hQE_2 contains two QE’s which are fermions indistinguishable from the third QE, the exclusion principle forbids the states with $L = 1$ and 2 ($L_{3QE} \leq \frac{15}{2}$ so that

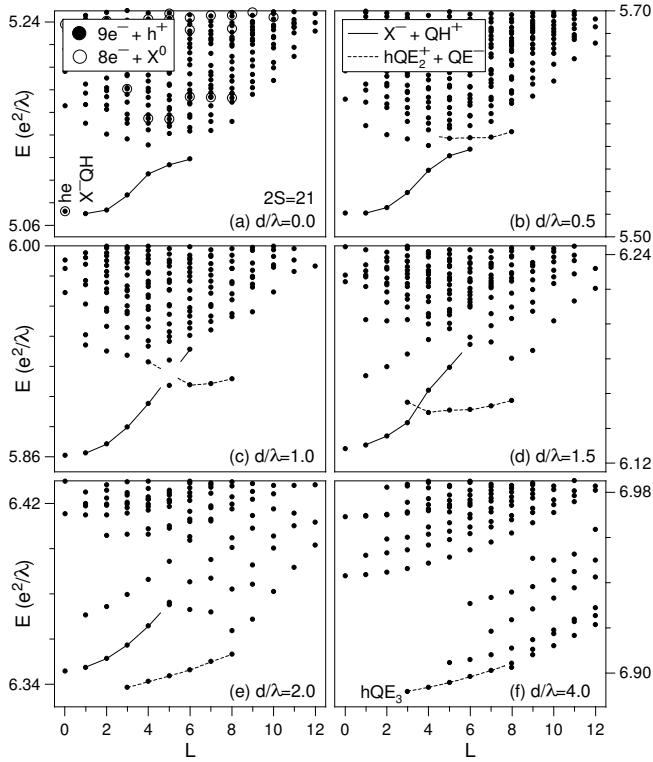


FIG. 10. The energy spectra (energy E vs. angular momentum L) of the $9e-h$ system calculated on a Haldane sphere with monopole strength $2S = 21$ for different layer separations d . The open circles mark the multiplicative states at $d = 0$. λ is the magnetic length.

adding it to $l_h = \frac{21}{2}$ cannot give $L < 3$). The resulting band at $L = 3, 4, \dots, 8$ indeed appears in the $9e-h$ spectrum at $\lambda \leq d \leq 2\lambda$. The dependence of E on L within this band is (up to a constant shift in energy) the hQE_2 -QE pseudopotential, $V_{hQE_2-QE}(L)$. Since hQE_2 and QE have opposite charge (opposite angular momentum), the decrease of V_{hQE_2-QE} as a function of L at $d \leq 1.5\lambda$ signals the hQE_2 -QE repulsion, consistent with the result in Fig. 8 that hQE_3 does not bind. At $d \geq 4\lambda$, the low energy bands contain low energy three-QE eigenstates weakly coupled (bound) to the hole. At $d = 4\lambda$, the lowest of those band contains the QE_3 molecule, with $l_{QE_3} \equiv 3l_{QE} - 3 = \frac{15}{2}$, and the ground state is hQE_3 at $l_{hQE_3} \equiv |l_h - l_{QE_3}| = 3$. At even much larger d , the ground state consist of the three-QE ground state (which for $N = 9$ at $2S = 21$ occurs at $L_{3QE} = \frac{5}{2}$) virtually decoupled from the hole. Note that the fact that hQE_3 is the $9e-h$ ground state in Fig. 10(e,f) does not mean that it is a stable bound complex in an infinite system. The comparison of binding energies in Figs. 8 and 14(b) shows that if only the third QE could move away from the hQE_2 (which it cannot do in a finite system in Fig. 10), the hQE_3 would unbind at any d .

$2S = 22$ (Fig. 11): At small d , the low energy states contain an X^- interacting with two QH's of the Laughlin $[3^*2]$ state of the $7e-X^-$ fluid. The angular momenta of

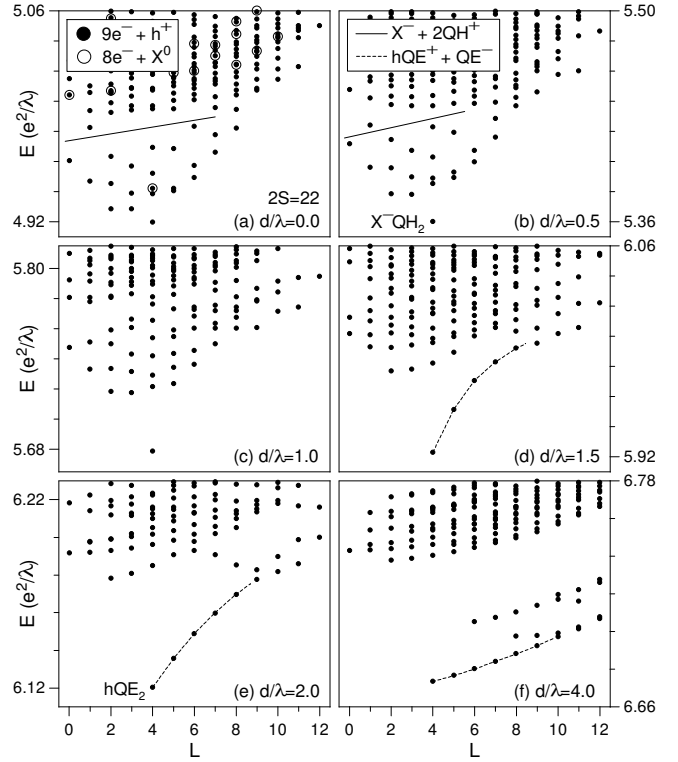


FIG. 11. The energy spectra (energy E vs. angular momentum L) of the $9e-h$ system calculated on a Haldane sphere with monopole strength $2S = 22$ for different layer separations d . The open circles mark the multiplicative states at $d = 0$. λ is the magnetic length.

an electron "quasihole" QH_e (that we will denote here simply by QH) and an X^- "quasielectron" QE_{X^-} (denoted simply by X^-) are obtained from the generalized CF picture: $l_e^* \equiv S - (N - 2) = 4$ and $l_{X^-}^* \equiv l_e^* - 1 = 3$. The two-QH states can have $L_{2QH} = 2l_e^* - \mathcal{R} = 1, 3, 5, \text{ or } 7$. Adding allowed L_{2QH} to $l_{X^-}^*$ gives allowed total X^- -2QH angular momenta $L = 0, 1, 2^2, 3^2, \dots, 9$, and 10. Indeed, these multiplets form the lowest energy band of states at $d \leq 0.5\lambda$ separated from higher states by solid lines in Fig. 11(ab).

The lowest state in this band (the $9e-h$ ground state) is the bound X^-QH_2 state, at angular momentum $l_{X^-QH_2} \equiv |l_{QH_2} - l_{X^-}^*| = 4$. The lowest MP state at $d = 0$ and $L = 4$ (marked with an open circle) has higher energy than X^-QH_2 . It contains a $k = 0$ exciton decoupled from one Laughlin QH of the eight electron system.

At $d > \lambda$, the low energy band of states develops at $L \geq 4$. These states contain an hQE interacting with the second QE (this interaction is attractive, because V_{hQE-QE} increases as a function of L , and hQE and QE have opposite charge). The lowest state is the bound hQE_2 state, whose angular momentum $l_{hQE_2} = 4$ results from addition of two $l_{QE} = 4$ to obtain $l_{QE_2} = 7$, and then adding to it $l_h = 11$. Note that because hQE_2 has the same angular momentum $L = \frac{1}{2}(N - 1)$ as X^-QH_2 , the transition from one state to the other is continuous.

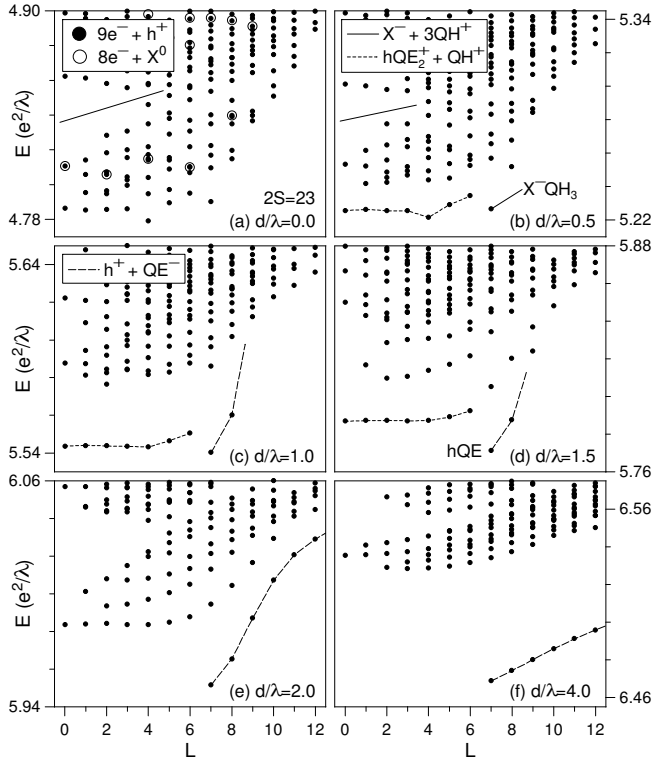


FIG. 12. The energy spectra (energy E vs. angular momentum L) of the $9e-h$ system calculated on a Haldane sphere with monopole strength $2S = 23$ for different layer separations d . The open circles mark the multiplicative states at $d = 0$. λ is the magnetic length.

It is apparent from the dependence of PL intensity⁴⁶ on d that it occurs about $d \approx 1.66\lambda$.

$2S = 23$ (Fig. 12): At small d , the low energy states contain an X^- interacting with three QH's of the Laughlin $[3^*2]$ state of the $7e-X^-$ fluid. The generalized CF picture uses $l_e^* \equiv S - (N - 2) = \frac{9}{2}$ and $l_{X^-}^* \equiv l_e^* - 1 = \frac{7}{2}$, and predicts $L = 1, 2^4, 3^6, \dots, 13$ for this band. Indeed, at least at small L , these X^- -3QH states can be identified in Fig. 12(ab). The angular momentum of a bound X^- -QH₃ results from adding three $l_{QH_3} = 3l_e^* - 3$ to $l_{X^-}^*$ to obtain $l_{hQH_3} = |l_{QH_3} - l_{X^-}^*| = 7$. Although most likely X^- -QH₃ is the lowest state at $L = 7$ in Fig. 12(a), it has higher energy than other states and thus it is unstable (due to the short range of QH-QH repulsion;⁵⁵ see also Fig. 6(f) for the QH-QH pseudopotential in a seven-electron system).

At $d > \lambda$, the X^- unbinds and the X^- -3QH band undergoes reconstruction. At $d \approx \lambda$, two competing low energy bands occur in the spectra in Fig. 12(bcd). One describes the hole with $l_h \equiv S = \frac{23}{2}$ and the QE with $l_{QE} \equiv S - (N - 1) + 1 = \frac{9}{2}$ interacting through a pseudopotential similar to that in Fig. 6(a). This band has $L \geq |l_h - l_{QE}| = 7$, and the lowest two states (at $L = 7$ and 8) are hQE and hQE^* . The second band involves an additional QE-QH pair and describes the hQE_2 with $l_{hQE_2} \equiv |l_h - l_{QE_2}| = |l_h - (2l_{QE} - 1)| = \frac{7}{2}$ interacting

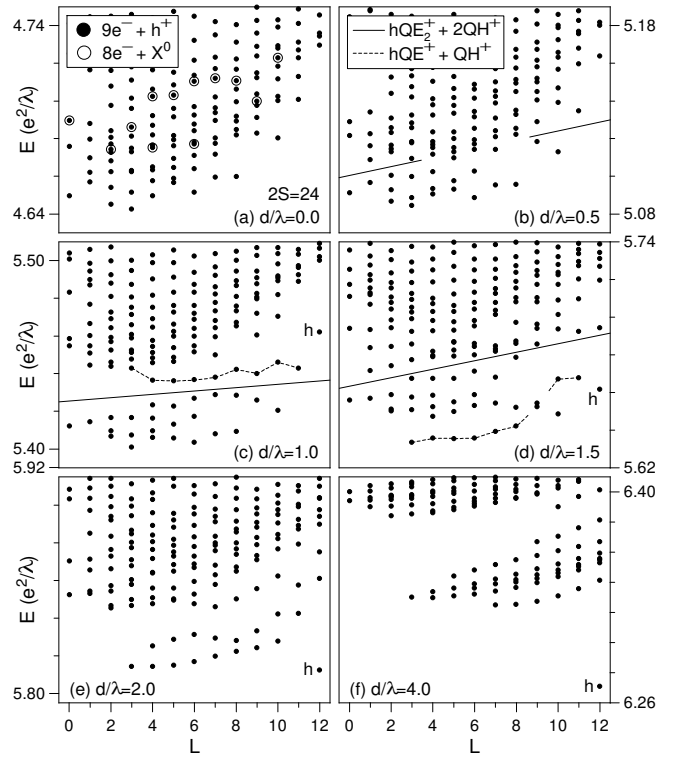


FIG. 13. The energy spectra (energy E vs. angular momentum L) of the $9e-h$ system calculated on a Haldane sphere with monopole strength $2S = 24$ for different layer separations d . The open circles mark the multiplicative states at $d = 0$. λ is the magnetic length.

with the QH with $l_{QH} \equiv S - (N - 1) = \frac{7}{2}$. The angular momenta L obtained by adding l_{hQE_2} and l_{QH} satisfy $|l_{hQE_2} - l_{QH}| \leq L \leq l_{hQE_2} + l_{QH}$, i.e. $0 \leq L \leq 7$. Because of the “hard core” of V_{QE-QH} (the QE-QH state at $L = 1$ does not occur⁴⁵), the hQE_2 -QH state at the highest value of L is forbidden, and the hQE_2 -QH band has $L = 0, 1, 2, \dots, 6$. We showed in Sec. VI that creation of an additional QE-QH pair to bind the second QE to hQE and form hQE_2 is energetically favorable at $d \leq \lambda$ (see the crossing of Δ_{hQE_2} and $2(\varepsilon_{QE} + \varepsilon_{QH})$ in Fig. 8). Indeed, in Fig. 12 the hQE state crosses the hQE_2 -QH band and becomes the $9e-h$ ground state at $d \approx \lambda$.

$2S = 24$ (Fig. 13): At small d , the lowest states contain an X^- interacting with four QH's of the $[3^*2]$ state of the $7e-X^-$ fluid. This band is fairly broad and overlaps with higher ones, containing additional QE-QH pairs.

In the $L \equiv S = 12$ ground state at very large d , the hole is decoupled from the $\nu = \frac{1}{3}$ state of $N = 9$ electrons. The excitation gap in Fig. 13(f) is the Laughlin gap of the 2DEG, and the first excited band describes the interaction of the hole with an additional QE-QH pair [$l_{QE} \equiv S - (N - 1) + 1 = 5$ and $l_{QH} \equiv S - (N - 1) = 4$], and it contains $L = 3, 4^2, 5^3, 6^4, 7^5, \dots$, resulting from adding $2 \leq L_{QE-QH} \leq 9$ to $l_h = 12$. At $d \approx 1.5\lambda$, the h -QE attraction exceeds both the magneto-roton energy (QE-QH attraction) and the $\varepsilon_{QE} + \varepsilon_{QH}$ gap, and the low-

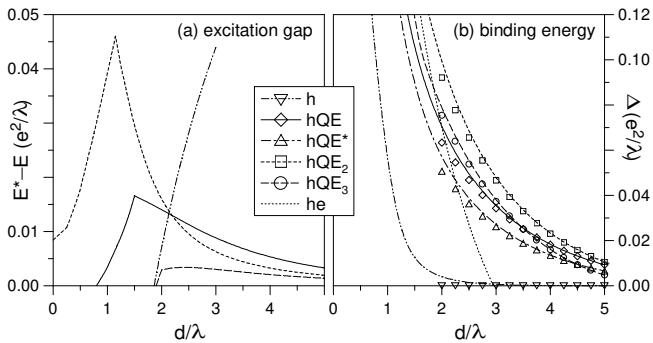


FIG. 14. The excitation gap $E^* - E$ (a), and binding energy Δ (b) of fractionally charged excitons hQE_n as a function of layer separation d , calculated for the $8e-h$ system. E_X is the exciton energy and λ is the magnetic length. The he state contains an exciton and originates from the multiplicative state at $d = 0$.

est energy band at $3 \leq L \leq 11$ in Fig. 13(d) contains a bound hQE state with $l_{hQE} \equiv |l_h - l_{QE}| = 7$ interacting with a QH. At $d \approx \lambda$, the $h-QE$ attraction becomes even stronger and the hQE_2 state with $l_{hQE_2} \equiv |l_h - l_{QE_2}| = 3$ is formed. The lowest band in Fig. 13(c) describes the interaction of an hQE_2 state with two QH's. The addition of l_{hQE_2} and two l_{QH} 's gives a band at $L = 0, 1, 2^3, \dots, 10$ observed in Fig. 13(c).

In Fig. 14 we present the data regarding the stability of different FCX's, extracted from the $8e-h$ spectra, similar those in Figs. 9–13. We have checked that the curves plotted here for $N = 8$ are very close to those obtained for $N = 7$ or 9 , so that all important properties of an extended system can be understood from a rather simple $8e-h$ computation. In two frames, for each hQE_n we plot: (a) the excitation gap $E^* - E$ above the hQE_n ground state, and (b) the binding energy Δ . The excitation gaps are obtained from the spectra at $2S = 3(N - 1) - n$ in which isolated hQE_n complexes occur. The binding energy Δ is defined in such way that $E_{hQE_n} = E_{QE_n} + V_{h-LS} - \Delta$, where E_{hQE_n} is the energy of the $Ne-h$ system in state hQE_n calculated at $2S = 3(N - 1) - n$, E_{QE_n} is the energy of the Ne system in state QE_n calculated at the same $2S = 3(N - 1) - n$, and V_{h-LS} is the self-energy of the hole in Laughlin $\nu = \frac{1}{3}$ ground state at $2S = 3(N - 1)$. As described in Sec. VI, V_{h-LS} is calculated by setting the hole charge to a very small fraction of $+e$ so that it does not perturb the Laughlin ground state.

The lines in Fig. 14 show data obtained from the spectra similar to those in Figs. 9–13, i.e. including all effects of $e-h$ interactions. For comparison, with symbols we have shown the data plotted previously in Fig. 8, where very small hole charge e/ϵ was used in the calculation to assure that, at any d , the obtained low energy eigenstates are given exactly by the hQE_n wavefunction. At $d > \lambda$, very good agreement between binding energies calculated for $\epsilon = 1$ (lines) and $\epsilon \gg 1$ (symbols) confirms our identification of hQE_n states in low energy $Ne-h$ spectra. At $d < \lambda$ the two calculations give quite different re-

sults which confirms that the description of actual $Ne-h$ eigenstates in terms of the hole interacting with Laughlin quasiparticles of the 2DEG is inappropriate (the correct picture is that of a two-component $e-X^-$ fluid).

The formation of hQE_n complexes at d larger than about 1.5λ can be seen most clearly in the dependence⁴⁶ of their PL intensity on d . Although d is the only tunable parameter in an $e-h$ system, the transition from “integrally” to “fractionally” charged exciton phase occurs in the phase space of two parameters, D and U , which define the perturbation potential V_{UD} . Different combinations of U and D are possible in systems where the hole is replaced by an electrode (STM) or a charged impurity.^{41,42} The relation between U and D in realistic $e-h$ systems depends somewhat on the magnetic field and electron density (because of the asymmetric inter-LL scattering for electrons and holes), and/or on the widths of electron and hole layers. We have calculated similar dependences to those in Fig. 14 for the $e-h$ interaction multiplied by a constant, $\epsilon^{-1}V_{eh}$, and found that the phase transition occurs in every case. The critical layer separation depends on ϵ and equals $d/\lambda = 0.84, 1.66, 2.25, 2.61,$ and 2.95 , for $\epsilon^{-1} = 0.5, 1, 1.5, 2,$ and 2.5 , respectively.

The analysis of the characteristics of hQE_n complexes plotted in Fig. 14 (and the good agreement of the actual binding energies with those obtained for $\epsilon \gg 1$) confirms that the most important bound complex to understand PL at $d \geq 2\lambda$ is hQE_2 , which has the largest binding energy Δ , and significant excitation energy $E^* - E$. The hQE is also a fairly strongly bound complex with large excitation energy, but the charge neutral “anyon exciton” suggested by Rashba et al.²⁷ is not bound. It will be shown in a subsequent publication,⁴⁶ the hQE_2 complex has a significant PL oscillator strength, while neither hQE nor hQE_3 are radiative. Finally, the radiative excitonic state (charge neutral $e-h$ pair weakly coupled to the 2DEG) breaks apart at $d > 2\lambda$.

VIII. CONCLUSION

Using exact numerical diagonalization, we have studied energy spectra of a 2DEG in the FQH regime interacting with an optically injected valence band hole confined to a parallel 2D layer. Depending on the separation d between the electron and hole layers, different response of the 2DEG to the hole has been found. At d smaller than a magnetic length λ , the hole binds one or two electrons to form neutral (X) or charged (X^-) excitons. The X 's are weakly coupled to the 2DEG, and the X^- 's with the remaining electrons form a two-component fluid with Laughlin correlations. One or two of the QH excitations of this fluid can bind to an X^- to form a X^-QH_n complex. The PL spectrum at small d depends on the lifetimes and binding energies of the X and X^- states, rather than on the original correlations of the 2DEG. No anomaly occurs in PL at the Laughlin filling factor

$\nu = \frac{1}{3}$, at which the FQH effect is observed in transport experiments.

At d larger than about 2λ , the Coulomb potential of the distant hole becomes too weak and its range becomes too large to bind individual electrons and form the X or X^- states. Instead, fractionally charged excitons hQE_n are formed, consisting of one or two Laughlin QE's bound to the hole. Different hQE_n complexes have different optical properties⁴⁶ (recombination lifetimes and energies), and which of them occur depends critically on whether QE's are present in the 2DEG. Hence, discontinuities occur in the PL spectrum at $\nu = \frac{1}{3}$.

The crossover between the “integrally” and “fractionally” charged exciton phases in an $e-h$ system can be viewed as a change in the response of a 2DEG to a more general perturbation potential V_{UD} defined in terms of its characteristic energy (U) and length (D) scales. An analogous transition will occur in other similar systems, in which the 2DEG is perturbed by a charged impurity^{41,42} or an electrode. However, a difference between the response to negatively and positively charged probes is expected because of very different QE-QE and QH-QH interactions at short range.

Our results invalidate two suggestive concepts proposed to understand the numerical $Ne-h$ spectra and the observed PL of a 2DEG. First, in contrast with the works of Wang et al.,²⁵ and Apalkov and Rashba,²⁶ we have shown that the “dressed exciton” states with finite momentum ($k \neq 0$) do not occur in the low energy spectra of $e-h$ systems at small d . The coupling of $k \neq 0$ excitons to the 2DEG is too strong to be treated perturbatively, and does more than renormalization of the exciton mass. Rather, it causes instability of $k \neq 0$ excitons and formation of charged excitons X^- . And second, we have shown in contrast with the work of Rashba and Portnoi,²⁷ that the charge-neutral “anyon excitons” hQE_3 are not stable at any value of d (they are also non-radiative⁴⁶).

ACKNOWLEDGMENT

The authors acknowledge partial support by the Materials Research Program of Basic Energy Sciences, US Department of Energy, and thank K. S. Yi (Pusan National University, Korea) who participated in the early stages of this study, and P. Hawrylak (National Research Council, Canada) and M. Potemski (High Magnetic Field Laboratory, Grenoble, France) for helpful discussions. AW acknowledges partial support from the Polish State Committee for Scientific Research (KBN) grant 2P03B11118.

- C. Gossard, and J. H. English, Phys. Rev. Lett. **61**, 605 (1988).
- ² A. J. Turberfield, S. R. Haynes, P. A. Wright, R. A. Ford, R. G. Clark, J. F. Ryan, J. J. Harris, and C. T. Foxon, Phys. Rev. Lett. **65**, 637 (1990).
- ³ B. B. Goldberg, D. Heiman, A. Pinczuk, L. N. Pfeiffer, and K. West, Phys. Rev. Lett. **65**, 641 (1990).
- ⁴ H. Buhmann, W. Joss, K. von Klitzing, I. V. Kukushkin, G. Martinez, A. S. Plaut, K. Ploog, and V. B. Timofeev, Phys. Rev. Lett. **65**, 1056 (1990); H. Buhmann, W. Joss, K. von Klitzing, I. V. Kukushkin, G. Martinez, K. Ploog, and V. B. Timofeev, *ibid.* **66**, 926 (1991).
- ⁵ E. M. Goldys, S. A. Brown, A. G. Davies, R. Newbury, R. G. Clark, P. E. Simmonds, J. J. Harris, and C. T. Foxon, Phys. Rev. B **46**, R7957 (1992).
- ⁶ I. V. Kukushkin, R. J. Haug, K. von Klitzing, K. Eberl, and K. Töttemeyer, Phys. Rev. B **50**, 11 259 (1994).
- ⁷ S. Takeyama, H. Kunimatsu, K. Uchida, N. Miura, G. Karczewski, J. Jaroszynski, T. Wojtowicz, and J. Kossut, Physica B **246-247**, 200 (1998); H. Kunimatsu, S. Takeyama, K. Uchida, N. Miura, G. Karczewski, T. Wojtowicz, and J. Kossut, *ibid.* **249-251**, 951 (1998).
- ⁸ L. Gravier, M. Potemski, P. Hawrylak, and B. Etienne, Phys. Rev. Lett. **80**, 3344 (1998).
- ⁹ A. Pinczuk, B. S. Dennis, L. N. Pfeiffer, and K. West, Phys. Rev. Lett. **70**, 3983 (1993).
- ¹⁰ K. Kheng, R. T. Cox, Y. Merle d'Aubigne, F. Bassani, K. Saminadayar, and S. Tatarenko, Phys. Rev. Lett. **71**, 1752 (1993).
- ¹¹ H. Buhmann, L. Mansouri, J. Wang, P. H. Beton, N. Mori, M. Heini, and M. Potemski, Phys. Rev. B **51**, 7969 (1995).
- ¹² A. J. Shields, M. Pepper, M. Y. Simmons, and D. A. Ritchie, Phys. Rev. B **52**, 7841 (1995).
- ¹³ G. Finkelstein, H. Shtrikman, and I. Bar-Joseph, Phys. Rev. Lett. **74**, 976 (1995); Phys. Rev. B **53**, R1709 (1996).
- ¹⁴ M. Hayne, C. L. Jones, R. Bogaerts, C. Riva, A. Usher, F. M. Peeters, F. Herlach, V. V. Moshchalkov, and M. Henini, Phys. Rev. B **59**, 2927 (1999).
- ¹⁵ H. A. Nickel, G. S. Herold, T. Yeo, G. Kioseoglou, Z. X. Jiang, B. D. McCombe, A. Petrou, D. Broido, and W. Schaff, Phys. Status Solidi B **210**, 341 (1998).
- ¹⁶ J. G. Tischler, B. A. Weinstein, and B. D. McCombe, Phys. Status Solidi B **215**, 263 (1999).
- ¹⁷ T. Wojtowicz, M. Kutrowski, G. Karczewski, J. Kossut, F. J. Teran, and M. Potemski, Phys. Rev. B **59**, R10 437 (1999).
- ¹⁸ Z. X. Jiang, B. D. McCombe, and P. Hawrylak, Phys. Rev. Lett. **81**, 3499 (1998).
- ¹⁹ S. A. Brown, J. F. Young, J. A. Brum, P. Hawrylak, and Z. Wasilewski, Phys. Rev. B **54**, R11 082(1996).
- ²⁰ Y. Kim, F. M. Munteanu, C. H. Perry, D. G. Rickel, J. A. Simmons, and J. L. Reno, Phys. Rev. B **61**, 4492 (2000); F. M. Munteanu, Y. Kim, C. H. Perry, D. G. Rickel, J. A. Simmons, and J. L. Reno, *ibid.* **61**, 4731 (2000).
- ²¹ I. V. Lerner and Yu. E. Lozovik, Zh. Eksp. Teor. Fiz. **80**, 1488 (1981) [Sov. Phys. JETP **53**, 763 (1981)].
- ²² A. B. Dzyubenko and Yu. E. Lozovik, Fiz. Tverd. Tela **25**, 1519 (1983) [Sov. Phys. Solid State **25**, 874 (1983)].
- ²³ A. H. MacDonald and E. H. Rezayi, Phys. Rev. B **42**, 3224 (1990).

¹ D. Heiman, B. B. Goldberg, A. Pinczuk, C. W. Tu, A.

- ²⁴ A. H. MacDonald, E. H. Rezayi, and D. Keller, Phys. Rev. Lett. **68**, 1939 (1992).
- ²⁵ B.-S. Wang, J. L. Birman, and Z.-B. Su, Phys. Rev. Lett. **68**, 1605 (1992).
- ²⁶ V. M. Apalkov and E. I. Rashba, Phys. Rev. B **46**, 1628 (1992); *ibid.* **48**, 18 312 (1993).
- ²⁷ E. I. Rashba and M. E. Portnoi, Phys. Rev. Lett. **70**, 3315 (1993); V. M. Apalkov, F. G. Pikus, and E. I. Rashba, Phys. Rev. B **52**, 6111 (1995); M. E. Portnoi and E. I. Rashba, *ibid.* **54**, 13 791 (1996).
- ²⁸ X. M. Chen and J. J. Quinn, Phys. Rev. Lett. **70**, 2130 (1993); Phys. Rev. B **50**, 2354 (1994); *ibid.* **51**, 5578 (1995).
- ²⁹ B. Stebe and A. Ainane, Superlatt. Microstruct. **5**, 545 (1989).
- ³⁰ A. Wójs and P. Hawrylak, Phys. Rev. B **51**, 10 880 (1995).
- ³¹ J. J. Palacios, D. Yoshioka, and A. H. MacDonald, Phys. Rev. B **54**, 2296 (1996).
- ³² A. Wójs, P. Hawrylak, and J. J. Quinn, Physica B **256-258**, 490 (1998); Phys. Rev. B **60**, 11 661 (1999).
- ³³ A. Wójs, I. Szlufarska, K. S. Yi, and J. J. Quinn, Phys. Rev. B **60**, R11 273 (1999).
- ³⁴ A. Wójs, J. J. Quinn, and P. Hawrylak, Physica E (to appear, e-print cond-mat/0001327); Phys. Rev. B (to appear, e-print cond-mat/0001328).
- ³⁵ D. M. Whittaker and A. J. Shields, Phys. Rev. B **56**, 15 185 (1997).
- ³⁶ P. Hawrylak, Phys. Rev. B **44**, 3821 (1991); J. A. Brum and P. Hawrylak, Comments Cond. Matt. Phys. **18**, 135 (1997).
- ³⁷ P. Hawrylak and M. Potemski, Phys. Rev. B **56**, 12 386 (1997).
- ³⁸ R. B. Laughlin, Phys. Rev. Lett. **50**, 1395 (1983).
- ³⁹ D. C. Tsui, H. L. Störmer, and A. C. Gossard, Phys. Rev. Lett. **48**, 1559 (1982).
- ⁴⁰ G. Binning and H. Rohrer, Rev. Mod. Phys. **59**, 615 (1987).
- ⁴¹ E. H. Rezayi and F. D. M. Haldane, Phys. Rev. B **32**, R6924 (1985); F. C. Zhang, V. Z. Vulovic, Y. Guo, and S. Das Sarma, *ibid.* **32**, R6920 (1985).
- ⁴² H. L. Fox and D. M. Larsen Phys. Rev. B **51**, 10 709 (1995); C. Riva, V. A. Schweigert, and F. M. Peeters, Phys. Rev. B **57**, 15 392 (1998).
- ⁴³ B. I. Halperin, Helv. Phys. Acta **56**, 75 (1983).
- ⁴⁴ F. D. M. Haldane, in “The Quantum Hall Effect” edited by R. E. Prange and S. M. Girvin, Springer, New York (1987), chapter 8, p. 303.
- ⁴⁵ A. Wójs and J. J. Quinn, Solid State Commun. **108**, 493 (1998); *ibid.* **110**, 45 (1999); Acta Phys. Pol. A **96** 403 (1999); Phil. Mag. B **80**, 1405 (2000); J. J. Quinn and A. Wójs, J. Phys.: Cond. Mat. **12**, R265 (2000).
- ⁴⁶ A. Wójs and J. J. Quinn, to be published.
- ⁴⁷ J. E. Avron, I. W. Herbst, and B. Simon, Ann. Phys. **114**, 431 (1978).
- ⁴⁸ A. B. Dzyubenko, Solid State Commun. **113**, 683 (2000).
- ⁴⁹ F. D. M. Haldane, Phys. Rev. Lett. **51**, 605 (1983).
- ⁵⁰ T. T. Wu and C. N. Yang, Nucl. Phys. B **107**, 365 (1976).
- ⁵¹ C. Lanczos, J. Res. Natn. Bur. Stand. **45**, 255 (1950).
- ⁵² A. Wójs and J. J. Quinn, Physica E **3**, 181 (1998).
- ⁵³ G. Fano, F. Ortolani, and E. Colombo, Phys. Rev. B **34**, 2670 (1986).
- ⁵⁴ E. H. Rezayi, Phys. Rev. B **36**, 5454 (1987); *ibid.* **43**, 5944 (1991); S. L. Sondhi, A. Karlhede, and S. A. Kivelson, and E. H. Rezayi, *ibid.* **47**, 16 419 (1993).
- ⁵⁵ A. Wójs and J. J. Quinn, Phys. Rev. B **61**, 2846 (1998).
- ⁵⁶ L. P. Gorkov and I. E. Dzyaloshinskii, Zh. Eksp. Teor. Fiz. **80**, 1488 (1981) [Sov. Phys. JETP **26**, 449 (1969)].
- ⁵⁷ S. N. Yi, X. M. Chen, and J. J. Quinn, Phys. Rev. B **53**, 9599 (1996).
- ⁵⁸ G. S. Canright, S. M. Girvin, and A. Brass, Phys. Rev. Lett. **63**, 2291 (1989); X. C. Xie, S. He, and S. Das Sarma, *ibid.* **66**, 389 (1991).
- ⁵⁹ A. J. Shields, F. M. Bolton, M. Y. Simmons, M. Pepper, and D. A. Ritchie, Phys. Rev. B **55**, 1970 (1997).